



저작자표시-비영리-변경금지 2.0 대한민국

이용자는 아래의 조건을 따르는 경우에 한하여 자유롭게

- 이 저작물을 복제, 배포, 전송, 전시, 공연 및 방송할 수 있습니다.

다음과 같은 조건을 따라야 합니다:



저작자표시. 귀하는 원저작자를 표시하여야 합니다.



비영리. 귀하는 이 저작물을 영리 목적으로 이용할 수 없습니다.



변경금지. 귀하는 이 저작물을 개작, 변형 또는 가공할 수 없습니다.

- 귀하는, 이 저작물의 재이용이나 배포의 경우, 이 저작물에 적용된 이용허락조건을 명확하게 나타내어야 합니다.
- 저작권자로부터 별도의 허가를 받으면 이러한 조건들은 적용되지 않습니다.

저작권법에 따른 이용자의 권리는 위의 내용에 의하여 영향을 받지 않습니다.

이것은 [이용허락규약\(Legal Code\)](#)을 이해하기 쉽게 요약한 것입니다.

[Disclaimer](#)

**A THESIS
FOR THE DEGREE OF MASTER OF SCIENCE**

**Dithiol Glutaredoxin Systems and Their Functional
Significance in Teleost Immune Responses; Deciphering Roles
of Glutaredoxin 1 and 2 in Redox Homeostasis of Big Belly
Seahorse (*Hippocampus abdominalis*)**

Welivitiye Kankanamge Malithi Omeka

**DEPARTMENT OF MARINE LIFE SCIENCES
GRADUATE SCHOOL
JEJU NATIONAL UNIVERSITY
REPUBLIC OF KOREA**

August 2019

Dithiol glutaredoxin systems and their functional significance in teleost immune responses; deciphering roles of glutaredoxin 1 and 2 in redox homeostasis of big belly seahorse (*Hippocampus abdominalis*)

Welivitiye Kankanamge Malithi Omeka

(Supervised by Professor Jehee Lee)

A thesis submitted in partial fulfilment of the requirement for the degree of

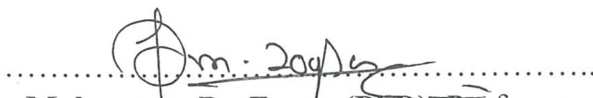
MASTER OF SCIENCE

August 2019

This thesis has been examined and approved by



Thesis director, **Sukkyoung Lee (PhD)**, Research Professor
Fish Vaccine Research Center, Jeju National University



Mahanama De Zoysa (PhD), Professor
College of Veterinary Medicine, Chungnam National University



Jehee Lee (PhD), Professor of Marine Life Sciences
School of Marine Biomedical Sciences, Jeju National University

Date: 29 / 05 / 2019

**DEPARTMENT OF MARINE LIFE SCIENCES
GRADUATE SCHOOL
JEJU NATIONAL UNIVERSITY
REPUBLIC OF KOREA**



CONTENTS

SUMMARY	V
ACKNOWLEDGMENT	VI
List of Figures	VII
List of Tables.....	VIII
BACKGROUND.....	1
1.1. Big-belly Seahorse (<i>Hippocampus abdominalis</i>).....	2
1.2. Diseases in seahorse	3
1.3. Oxidative stress	4
1.4. Antioxidant system against oxidative stress.....	4
1.5. Glutaredoxin.....	5
1.6. Dithiol glutaredoxin system	6
1.7. Deglutathionylation and functions of dithiol glutaredoxin	6
1.8. Hypothesis and objectives of the present study.....	7
CHAPTER 1.....	9
2.1. Introduction	10
2.2. Materials and Methods.....	12
2.2.1. Identification of Grx1 from <i>H. abdominalis</i>	12
2.2.2. Bioinformatic analysis of HaGrx1 sequences	12
2.2.3. Sample collection for tissue-specific distribution and temporal expression analysis	13
2.2.4. RNA extraction and cDNA synthesis.....	14
2.2.5. Quantitative real-time PCR (qPCR) analysis	14
2.2.6. Statistical analyses of qPCR data	15
2.2.7. Recombinant plasmid construction	15
2.2.8. Overexpression and purification of HaGrx1 fusion protein.....	16
2.2.9. Functional assays.....	17
2.2.9.1. Dehydroascorbic (DHA) reductase assay.....	17
2.2.9.2. Relative DHAR activity of HaGrx1 with different thiol compounds.....	17
2.2.9.3. β -Hydroxyethyl Disulfide (HED) and reduction assay	18
2.2.9.4. Turbidimetric assay of insulin disulfide reduction.....	18
2.3. Results.....	18
2.3.1. Sequence analysis of HaGrx1	18
2.3.2. Tissue distribution and immune challenge.....	22
2.3.3. Expression and purification of rHaGrx1	24
2.3.4. Functional studies.....	25

2.3.4.1. Dehydroascorbic (DHA) reduction assay.....	25
2.3.4.2. Relative DHAR activity of HaGrx1 with different thiol compounds.....	25
2.3.4.3. HED reduction assay.....	27
2.3.4.4. Turbidimetric assay of insulin disulfide reduction.....	27
2.4 Discussion	29
CHAPTER 2.....	37
3.1. Introduction.....	38
3.2. Materials and methods	39
3.2.1. Identification and bioinformatic analysis of Grx2 sequence from <i>Hippocampus abdominalis</i>	39
3.2.2. Acclimatization of big- belly seahorses, tissue sampling and immune stimulation.....	40
3.2.3. RNA isolation and cDNA synthesis.....	41
3.2.4. The mRNA expression profiling by Quantitative real-time PCR (qPCR) analysis	41
3.2.5. Recombinant plasmid construction	42
3.2.6. Overexpression and purification of recombinant HaGrx2	42
3.2.7. Functional assays.....	43
3.2.7.1. HaGrx2 deglutathionylation activity corresponds to the Human Grx1	43
3.2.7.2. Oxidoreductase activity of HaGrx2.....	43
3.2.7.3. Cell culture and transfection of HaGrx2	44
3.2.7.4. Cell viability assay upon H ₂ O ₂	45
3.3. Results.....	45
3.3.1. Bioinformatic analysis of HaGrx2	45
3.3.2. Spatial and temporal expression profile of HaGrx2	49
3.3.3. Overexpression and purification of rHaGrx2 as MBP fusion protein.....	51
3.3.4 Functional studies.....	52
3.3.4.1. The deglutathionylation activity of rHaGrx2 correspond to the human Grx1	52
3.3.4.2. Oxidoreductase activity of rHaGrx2	52
3.3.4.3. Cytoprotective activity upon oxidative stress	54
3.4. Discussion	54
References.....	62

SUMMARY

Glutaredoxins (Grx) are redox enzymes conserved in viruses, eukaryotes, and prokaryotes. In this study, we characterized glutaredoxin 1 (HaGrx1) and glutaredoxin2 (HaGrx2) from big-belly seahorse, *Hippocampus abdominalis*. *In-silico* analysis showed that HaGrx1 contained the classical glutaredoxin 1 structure with a CSYC thioredoxin active site motif. HaGrx2 possess Glutaredoxin 2 structure with CPYC active site. According to multiple sequence alignment and phylogenetic reconstruction, HaGrx1 and HaGrx2 presented the highest homology to the Grx1, and Grx2 ortholog from *Hippocampus comes* respectively. Transcriptional studies demonstrated the ubiquitous distribution of *HaGrx1* and *HaGrx2* transcripts in all the seahorse tissues tested. HaGrx1 represented the highest expression in muscles whereas HaGrx2 highly expressed in brain and skin. Significant modulation ($p < 0.05$) of *HaGrx1* and *HaGrx2* transcripts were observed in blood as well as in liver upon stimulation with pathogen-associated molecular patterns and live pathogens. The β -hydroxyethyl disulfide reduction assay confirmed the antioxidant activity of recombinant HaGrx1. Further, dehydroascorbate reduction and insulin disulfide reduction assays revealed the oxidoreductase activity of HaGrx1 and HaGrx2. HaGrx1 utilized 1,4-dithiothreitol, L-cysteine, 2-mercaptoethanol, and reduced L-glutathione as reducing agent with different dehydroascorbate reduction activity levels. HaGrx2 represented 84% activity that of human glutaredoxin1. Further, HaGrx2 exhibit antiapoptotic activity against H_2O_2 induced oxidative stress. Altogether, our results suggested a vital role of HaGrx1 and HaGrx2 in redox homeostasis as well as the host innate immune defense system.

ACKNOWLEDGMENT

This dissertation becomes a reality with the help and support of many individuals. I would like to extend my sincere gratitude to all of them.

Foremost, I would like to express gratefulness to my research supervisor Professor Jehee Lee, who gave me this opportunity to commence my post-graduate studies at Marine Molecular Genetics Lab, Jeju National University and supported me to be strong and work independently. I acknowledge him for his guidance for me in the scientific field and a better future.

Besides my supervisor, I would like to thank my thesis advisor Dr. Sukkyoung Lee and Dr. Mahanama De Zoysa for being my committee members.

Further, I am especially grateful to Dr. Gelshan Godahewa and Dr. Thiunuwan Priyathilaka, Dr. Seongdo Lee, Mr. Neranjan Tharuka for their valuable guidance and suggestions to improve my laboratory experiments and writings.

I would like to thank all the past and present lab members: Dr. Changnam Jin, Mr. Changyong Lim, Ms. Gabin Kim, Dr. Sang Phil Shin, Dr. Qiang Wan, Dr. Myoung-Jin Kim, Dr. Ms. Sumi Jung, Mr. Hyukjae Kwon, Ms. Hyerim Yang, Ms. Gayashani Sandamalika, Ms. Jeongeun Kim, Mr. Hanchang Sohn, Mr. Thilina Kasthuriarachchi, Mr. Nimod Dilushan, Mr. Kalana Prabhath, Mr. Kasun Madusanka, Ms. Chaehyeon Lim, Ms. Anushka Samaraweera, Ms. Sarithaa Sellaththurai, Mr. Jaewon Kim, Mr. Sudeera Shanaka, Mr. Srinith Prabhatha, Ms. Jayamini Harasgama, Ms. Kishanthini Nadarajpillai, for helping and encouraging me in various ways to complete my laboratory works.

I would like to thank my husband (Mr. Dileepa Liyanage) for his love, guidance and constant support in lab experiments and always been with me at difficult situations. This accomplishment would not have been without him.

Finally, my sincere thanks to all the funding authorities (Ministry of Oceans and Fisheries, Jeju National University, Korea) for providing research grants to accomplish the lab experiments.

List of Figures

Figure 1: Nucleotide and deduced amino acid sequence of HaGrx1 from <i>Hippocampus abdominalis</i>	19
Figure 2: Predicted tertiary structure of HaGrx1.	20
Figure 3: (A) multiple sequence alignment and (B) phylogenetic reconstruction of HaGrx1	21
Figure 4: (A) Tissue-specific expression of HaGrx1 and (B) Temporal expression profiles of HaGrx1 in the blood after immune stimulation.....	23
Figure 5: SDS-PAGE figure of rHaGrx1	24
Figure 6: (A) DHA reduction activity of rHaGrx1 with different DHA concentration and (B) with different GSH concentration	26
Figure 7: HED reduction activity of rHaGrx1 with different GSH concentrations at 25°C	27
Figure 8: Insulin disulfide reduction activity of rHaGrx1 with different protein and GSH combinations.	28
Figure 9: Sequence figure of HaGrx2	46
Figure 10: predicted amphipathic helix and predicted tertiary structure of HaGrx2	47
Figure 11: multiple sequence alignment of Grx2 orthologs.....	48
Figure 12: Phylogenetic reconstruction of HaGrx2	49
Figure 13: Tissue-specific expression profiles of HaGrx2.....	50
Figure 14: Temporal expression profiles of HaGrx2 in blood and liver	51
Figure 15: SDS-PAGE analysis of overexpressed HaGrx2 in <i>E. coli</i>	52
Figure 16: Insulin aggregation and dehydroascorbic acid reduction activity of rHaGrx2	53
Figure 17: percentage cell viability upon H ₂ O ₂ stress.	54

List of Tables

Table 1: Primers used for cloning and quantitative real-time PCR.....	16
Table 2: Identity and similarity percentages of Grx1 orthologs from different species compared to HaGrx1	22
Table 3: <i>Kinetic parameters of rHaGrx1 for DHA and HED assays at 25 °C.</i> The experiment was conducted in triplicates and data represent mean \pm SD.....	25
Table 4: Primers used in cloning and qRT-PCR of HaGrx2	44
Table 5: Identity and similarity percentages of HaGrx2 with other Grx2 orthologs from different species	48

BACKGROUND

1.1. Big-belly Seahorse (Hippocampus abdominalis)

Seahorses are considered as teleost (bony fish) that belongs to family Syngnathidae (Lourie et al., 2004). Pipefish, pipehorses, and seadragons also included in family Syngnathidae other than seahorses (Browne et al., 2008). This family has characteristic features such as male brood pouch, semi-flexible body encased in bony rings, tubular snout with a tiny mouth, absence of pelvic fins, etc. (Woods, 2007). Seahorses belong subfamily Hippocampinae which have a prehensile tail, fully enclosed brood pouch, and head angled ventrally from the abdominal axis (Lourie et al., 2004). The genus *Hippocampus* comprise with more than 70 species and can be found in marine and estuarine waters.

Big-belly seahorse (*Hippocampus abdominalis*) is the largest seahorse species identified and grow length up to 35 cm (Woods, 2007). Naturally, they can be found in tropical and temperate shallow coastal areas and habituated in the substrate such as mangroves and seagrasses where they can anchor by prehensile tails or sandy-muddy bottoms. They are known as carnivorous, and voracious feeders mainly depend on crustaceans (Woods, 2003).

Seahorses are mainly used for traditional Chinese medicine (TCM) (Bako, 2001). It is believed that dried seahorses in combination with other medicinal materials decrease cholesterol level, cure asthma, arthritis, gastritis, kidney and skin disorders (Woods, 2007). Recently, seahorses use as ornamental fish species and a large number of dead seahorses sold around the world as an object of curiosity. Key ring, jewelry, paperweight made from dead seahorse are famous in the USA. However, the majority of seahorse trade around the world are captured from the wild (Koldewey and Martin-Smith, 2010a).

Overexploitation from the wild by direct fishing and non-selective fishing gears made a significant negative impact on the seahorse population. They have limited distribution, low mobility and unique habitats which make them vulnerable in environmental pollution. Further, they have limited reproductive ability, lengthy parental care, mate fidelity with compared to other species, and it makes population instability in the natural environment (Woods, 2007). Out of 33 species, 25 seahorse species consider as data deficient, 7 as vulnerable and 1 as endangered according to the

IUCN Red list (Lourie et al., 2004). Further, all the seahorse species are conserved under CITES Appendix II. Based on the above facts, many countries permitted to farm *H. abdominalis* and cultured species are not subjected to restrictions of CITES.

1.2. Diseases in seahorse

Less growth of seahorses in aquaculture compared to the wild is one of a significant problem, but *H. abdominalis* showed similar growth rates at similar temperatures. However, almost all the farming seahorse species exhibit less tolerance for higher densities which made them vulnerable to infections and stress. Bacteria and parasites are commonly identified as threats for seahorses. *Mycobacterium spp.* such as *M. chelonae*, *M. fortuitum* and *M. marinum* can cause skin ulcerations, inflammation that leads to neurological defects and organ failure. Vibriosis caused by *Vibrio harveyi*, *V. alginolyticus*, and *V. splendidus* clinically identified as hemorrhagic to necrotic skin lesions in seahorses.

Parasites such as scuticociliates; unicellular eukaryotic marine organisms which cause scuticociliatosis has been identified in seahorses. Mainly, *Uronema marinum* and *Philasterides dicentrarchi* and *Cryptocaryon irritans* cause invasive ulcers and lesions in the skin and gill that leads to inflammation in the muscle, connective tissues, viscera, and coelomic cavity. *Trichodina sp.* also acts as an opportunistic pathogen for seahorses which cause for mild epithelial hyperplasia.

Fungal attacks such as Microsporidiosis cause by *Glugea heraldi* has been identified from *Hippocampus erectus*. Microsporidiosis make multifocal cysts in the skin that eventually rupture and leads to secondary bacterial infections.

Apart from the infections, ingestion of gas bubbles into gut significantly affect the survival rates of reared juvenile seahorses. They accidentally engulf the air when missing the food while praying on live food. The juveniles unable to release engulfed air out and exhibit irregular swimming, loss their balance, unable to capture the pray eventually leading to starvation and death. External gas bubble disease caused by the dissolved environment air in cultured systems or carbon dioxide produced by trapped bacteria in seahorse skin. Supersaturated oxygen and nitrogen in water diffused

into body fluids through membranes of yolk sacs, gills, and eyes. The gas bubbles formed in capillaries and under the skin, limit the blood flow and form clots.

There are many infections and disease identified in seahorse, but the clinical significance of diseases, treatments and inherent immune system of seahorses need to be explored further for successful disease prevention strategies.

1.3. Oxidative stress

Oxidative stress occurs when there is an imbalance between ROS and their antioxidants. ROS include oxygen free radicals such as hydroxyl, alkoxy, peroxy radicals and superoxide anions. Further, non-radical substances such as hydrogen peroxide, hypochlorous acid, and transition metals. Reactive oxygen species (ROS) and free radicals can be produced by three main sources. Electron transport in the mitochondrial respiratory chain is a primary ROS formation source within the cell. During the pathogenic invasion, immune cells such as neutrophils, monocytes, macrophages, dendritic cells, and B-lymphocyte form ROS as a strategy for pathogen destruction. ROS are generated by different environmental factors such as diet, radiation, and pollutants. However, these components have both benefits and pitfalls for defense mechanism in an organism. They can damage proteins, enzymes, carbohydrates, and lipid of cell compartments in excess levels, but on the other hand, ROS are essential for activating cellular pathways and energy production. Hence homeostasis of ROS and antioxidants is more essential on living organisms.

1.4. Antioxidant system against oxidative stress

Seahorse is not a primitive fish but an advance teleost which have well developed an innate and adaptive immune system similar to mammals. For the regulation of redox balance, cells are equipped with an antioxidant system comprised of non-enzymatic antioxidant molecules and antioxidant enzymes. Nonenzymatic antioxidant molecules can be produced endogenously or by dietary intake. Glutathione (GSH) is the most abundant nonenzymatic endogenous antioxidant molecule that produces only in the cytosol but distributed all over the cell. GSH reacts directly with

radical and neutralized them but also serve as an electron donor or antioxidant enzymes. Vitamins and minerals from dietary materials are the main exogenous antioxidant molecules in living organisms. Carotenoids, lipoic acid, ubiquinol, flavonoids, uric acids, ascorbic acid, vitamin E as well as minerals such as selenium and zinc act as ROS scavengers.

Antioxidant enzymes can be categorized into two groups; non-thiol antioxidant enzymes and thiol antioxidant enzymes. Superoxide dismutase (SOD) and catalase are the major non-thiol enzymes. Superoxide dismutase catalyzes the superoxide anions to hydrogen peroxide and oxygen. Catalase located in peroxisomes and convert hydrogen peroxide into water and oxygen.

Thioredoxins, peroxiredoxin, and glutaredoxin are the key thiol antioxidant enzymes can be found in cells. Thioredoxins first identified as a critical cofactor for ribonuclease reductase. Thioredoxin act as a system that comprises with NADPH and thioredoxin reductase. The primary function of peroxiredoxin is to detoxify hydroperoxides and hydrogen peroxide. Oxidized peroxiredoxins are reduced by thioredoxins.

1.5. Glutaredoxin

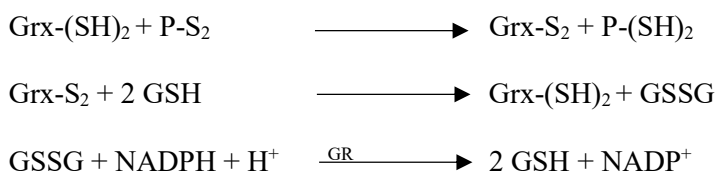
Glutaredoxins (Grxs) are known as glutathione-dependent thiol-disulfide oxidoreductases that are ubiquitously distributed in all living organisms (Bräutigam et al., 2013). They are small enzymes that belong to the thioredoxin superfamily but exhibit more versatile substrate activity than thioredoxins (Trxs) (Vlami-Gardikas and Holmgren, 2002). Grx family proteins have several isoforms with quite different structures and catalytic activities. They regulate essential and distinct biological functions in organisms.

Grxs can be classified into three categories based on their structure and catalytic properties. The first group is classical Grxs with a CXXC active site motif (usually CPYC) and a thioredoxin/glutaredoxin fold. Most vertebrate dithiol Grxs are included in this category. Members of the second category are structurally related to glutathione S-transferase but possess glutaredoxin oxidoreductase activity (Fernandes and Holmgren, 2004). A two-domain structure characterizes this category; the first domain contains a thioredoxin/glutaredoxin fold with CXXC and the second

domain has an α -helical structure (Vlami-Gardikas and Holmgren, 2002). Grx2 from *E. coli* is representative of this category. The third category is defined as monothiol Grx which is represented by a monothiol active site (Normally CGFS) (Lillig et al., 2008). Grx3, Grx4, and Grx5 from *Saccharomyces cerevisiae* belong to this category (Herrero et al., 2006). Further, the human protein kinase C-interacting cousin of thioredoxin (PICOT) is considered a monothiol Grx that belongs to the third category (Haunhorst et al., 2010).

1.6. Dithiol glutaredoxin system

Dithiol Grx contains CXXC thioredoxin catalytic motif as the leading active site. Most common active sites in dithiol Grx are CPYC or CSYC. Grx system comprises Grx, glutathione reductase, and GSH. In dithiol catalytic mechanism, N-terminal thiol group of Grx initiate a nucleophilic attack on one thiol group of targets and produce mixed disulfide between Grx and target molecule. Then C-terminal thiol of Grx active site, get deprotonated and attack the N-terminal thiol group of Grx that bonded with target disulfide. Consequently, oxidized Grx and reduced target molecule generated. This reaction generates an oxidized Grx which subsequently reduce to a dithiol by two GSH molecules and produce GSSG. Glutathione reductase (GR) utilize NADPH as an electron donor and regenerate GSH from GSSG.



1.7. Deglutathionylation and functions of dithiol glutaredoxin

The cysteine residues of proteins can undergo modifications during oxidative stress. Oxidation of cysteine residues generate sulfenic (RSOH), sulfinic (RSO₂H) and sulfonic (RSO₃H) acids. Sulfinate and sulfonate considered to be irreversible. Therefore, proteins susceptible to irreversible oxidation. However, a mild oxidative level can modify protein thiol groups and produce sulfenic acid while neighbor protein thiols may form disulfide bonds between each other or GSH. The process GSH attached to cysteine groups of protein is called glutathionylation. Glutathionylated

proteins have altered activity or structure compared to original protein. Glutathionylation protects the proteins from irreversible oxidation as well as activate many signaling pathways. Further, it can inactivate proteins such as transcription factor nuclear factor 1 (NF1), phosphofructokinase, and protein tyrosine phosphatase-1B (PTP1B). Further, modify the activity of protein kinase A (PKA), Protein kinase B (AKT), protein kinase C (PKC) and apoptosis signal-regulating kinase 1 (ASK1). Therefore, recovering of reduced protein is essential for the regulation of normal cell functions. Glutathionylation of proteins mainly reverses by glutaredoxin and this process called as deglutathionylation. Both glutathionylation and deglutathionylation are essential for redox homeostasis of cells but Grx capable of actively involved in cellular signaling cascades due to deglutathionylation.

Further, Grx can reduce low molecular weight disulfides such as coenzyme A, S-sulfocysteine, hydroxyethyl disulfide, L- cysteine, GSH, insulin, and cystamine. Moreover, it is reported that Grx can reduce mixed disulfides of papain, bovine serum albumin, and hemoglobin.

Apart from that, it is reported that Grx has bound [2Fe-2S] cofactor. Studies revealed that two other cysteine opposite to the active site of Grx coordinate the [2Fe-2S] cluster to make homodimers between two Grx molecules. Therefore, iron-sulfur cluster assembly is known as the physiological function of Grx. Further, Grx have dehydroascorbic reductase activity thus involve in ascorbic acid metabolism.

1.8. Hypothesis and objectives of the present study

Grx activity has been highly studied in eukaryotes (Mieyal and Gravina, 1993), prokaryotes (Vlami-Gardikas et al., 1997), and viruses (Rajagopal et al., 1995). However, there are few reports about Grx activity related to fish immunity and redox homeostasis. Only Grx2 from zebrafish was investigated for its role in Fe/S cluster coordination, brain development, and heart development (Berndt et al., 2014; Brautigam et al., 2011; Bräutigam et al., 2013). Moreover, transcriptional modulation of Grx1 and Grx2 from Manila clam were reported (Mu et al., 2012). However, there

have been no functional studies on Grx1 in teleost to date. Further, limited studies of Grx2 related to fish immunity are available.

Seahorses are a group of aquatic animals that have exploited for years for their medicinal and ornamental properties. Big-belly seahorse (*Hippocampus abdominalis*) is the largest seahorse species and is naturally distributed in the Korean peninsula and around the ocean [19]. Being a large, smooth-skinned species provides a high market value for big-belly seahorses. However, fulfilling the demand for seahorses is still a problem as they are extremely difficult to culture. One of the significant threats for seahorse cultivation is their poor adaptability to higher densities and stressful environments, thus increasing their vulnerability to pathogenic infections (Woods, 2007). Therefore, understanding the immune responses of big-belly seahorse against bacterial and pathogen-associated molecular pattern (PAMP) stimuli as well as assessing the functional aspects will facilitate the development and maintenance in seahorse cultivation. Accordingly, the present study investigated the molecular, transcriptional, and functional properties of Grx1 and Grx2 from big-belly seahorse (HaGrx1 and HaGrx2) to understand its role in immunity and redox homeostasis.

CHAPTER 1

**Glutaredoxin 1 from big-belly seahorse (*Hippocampus abdominalis*):
Molecular, transcriptional, and functional evidence in teleost immune
responses**

2.1. Introduction

Glutaredoxins (Grxs) are known as glutathione-dependent thiol-disulfide oxidoreductases that are ubiquitously distributed in all living organisms (Bräutigam et al., 2013). They are small enzymes that belong to the thioredoxin superfamily but exhibit more versatile substrate activity than thioredoxins (Trxs) (Vlamiš-Gardikas and Holmgren, 2002). Grx family proteins have a number of isoforms with quite different structures and catalytic activities. They regulate essential and distinct biological functions in organisms.

Grxs can be classified into three categories based on their structure and catalytic properties. The first group is classical Grxs with a CXXC active site motif (usually CPYC) and a thioredoxin/glutaredoxin fold. Most vertebrate dithiol Grxs are included in this category. Members of the second category are structurally related to glutathione S-transferase but possess glutaredoxin oxidoreductase activity (Fernandes and Holmgren, 2004). This category is characterized by a two-domain structure; the first domain contains a thioredoxin/glutaredoxin fold with CXXC and the second domain has an α -helical structure (Vlamiš-Gardikas and Holmgren, 2002). Grx2 from *E. coli* is representative of this category. The third category is defined as monothiol Grx which is represented by a monothiol active site (Normally CGFS) (Lillig et al., 2008). Grx3, Grx4, and Grx5 from *Saccharomyces cerevisiae* belong to this category (Herrero et al., 2006). Further, the human protein kinase C-interacting cousin of thioredoxin (PICOT) is considered a monothiol Grx that belongs to the third category (Haunhorst et al., 2010).

Grxs are versatile oxidoreductases that reduce various substrates such as H₂O₂, ribonucleotide reductase, dehydroascorbate, arsenate reductase, and others (Fernandes and Holmgren, 2004; Lillig et al., 2008). The typical Grx catalytic mechanism is similar to that of Trxs, which catalyze thiol-disulfide exchange using the CXXC motif, but Grx depends on GSH as an electron donor (Selles et al., 2009). Many of the substrates utilized by Grxs are essential to DNA synthesis, collagen synthesis, and maintain redox homeostasis (Lillig et al., 2008). Further, Grxs have been identified as a universal iron-sulfur cluster (Fe/S-cluster) coordinating proteins (Selles et

al., 2009). Fe/S-clusters are inorganic cofactors that facilitate electron transfer reactions, redox reactions, and protein folding (Bräutigam et al., 2013).

Regarding immunity, Grxs play a vital role in both viruses and humans. For example, Phage T4, *Vaccinia*, *Ectromelia*, and smallpox viruses produce their Grx that is essential for DNA synthesis, disulfide bond formation, and virus assembly (Hauwer, n.d.; Rajagopal et al., 1995; Vlamis-Gardikas and Holmgren, 2002). Additionally, human Grx1 regulates the activity of HIV-1 protease activity and thus is vital for regulating protease activity in HIV-1-infected cells (Davis et al., 1997). Moreover, Grxs demonstrated a crucial role in defending cardiomyocytes from oxidative stress by regulating the NF- κ B pathway (Ouchi and Walsh, 2012). In lung epithelial cells, Grx1 acts against bacterial infections by promoting S-glutathionylation of NF- κ B family proteins (Peltoniemi, 2007). Further, Grxs play an essential role in the nervous system and reproduction system in mammals (Daily et al., 2001; González-Fernández et al., 2005; Stavreus-Evers et al., 2002; Takagi et al., 1999).

Grx activity has been highly studied in eukaryotes (Mieyal and Gravina, 1993), prokaryotes (Vlamis-Gardikas et al., 1997), and viruses (Rajagopal et al., 1995). For example, Grxs from mammals and *E.coli* have been studied for their oxidoreductase activity (Mieyal and Gravina, 1993; Wells et al., 1990; Zahedi Avval and Holmgren, 2009) and thiyl radical scavenging and transferase properties of human Grx have been examined (Starke et al., 2003). However, there are few reports about Grx activity related to fish immunity and redox homeostasis. Only Grx2 from zebrafish was investigated for its role in Fe/S cluster coordination, brain development, and heart development (Berndt et al., 2014; Brautigam et al., 2011; Bräutigam et al., 2013). Moreover, transcriptional modulation of Grx1 and Grx2 from Manila clam were reported (Mu et al., 2012). However, there have been no functional studies on Grx1 in teleosts to date.

Seahorses are a group of aquatic animals that have exploited for years for their medicinal and ornamental properties. Annually, around 20 million seahorses are collected from the wild for medicinal purposes alone (Vincent, 1996). Therefore, seahorses have been included in global conservation programs (CITES) and cultivated for commercial use by many countries including Australia and Indonesia (Koldewey and Martin-Smith, 2010a; Vincent, 1996). Big-belly seahorse

(*Hippocampus abdominalis*) is the largest seahorse species and is naturally distributed in the Korean peninsula and around the ocean [19]. Being a large, smooth-skinned species provides a high market value for big-belly seahorses. However, fulfilling the demand for seahorses is still a problem as they are extremely difficult to culture. One of the significant threats for seahorse cultivation is their poor adaptability to higher densities and stressful environments, thus increasing their vulnerability to pathogenic infections (Woods, 2007). Therefore, understanding the immune responses of big-belly seahorse against bacterial and pathogen-associated molecular pattern (PAMP) stimuli will facilitate the development and maintenance in seahorse cultivation. Accordingly, the present study investigated the molecular, transcriptional, and functional properties of Grx1 from big-belly seahorse (HaGrx1) to understand its role in immunity.

2.2. Materials and Methods

2.2.1. Identification of Grx1 from *H. abdominalis*

The cDNA sequence with the highest homology to Grx1 was obtained from the big-belly seahorse transcriptomic database which was established previously (Oh et al., 2016). National Center for Biotechnology Information (NCBI) BLAST algorithm and RefSeq non-redundant protein databases were used to compare and verify the obtained sequence (Agarwala et al., 2016).

2.2.2. Bioinformatic analysis of HaGrx1 sequences

The coding sequence of HaGrx1 was obtained using the NCBI ORF Finder (<https://www.ncbi.nlm.nih.gov/orffinder/>), and putative polypeptide sequence was derived. Then, the amino acid sequence was verified using the NCBI blastp program (Agarwala et al., 2017). ExPASy ProtParam (Wilkins et al., 1999) was used to study the physiochemical properties of the HaGrx1 protein and predicted N-linked glycosylation sites were recognized by NetNGlyc 1.0 server (Gupta and Brunak, 2001). Further, signal peptides of HaGrx1 were analyzed by the SignalP 4.1 online tool (Petersen et al., 2011). The domain organization and signature motifs in the HaGrx1 amino acid sequence were analyzed by the NCBI conserved domain database (Marchler-Bauer et al.,

2015) and Motif Scan (Pagni et al., 2007). The SWISS model workbench (Biasini et al., 2014) was used to predict the tertiary structure of HaGrx1 by comparison with the crystal structure of human glutaredoxin 1 in its fully reduced form as a template (PDB; jhb.1). The predicted three-dimensional structure of the HaGrx1 protein was pictured by using PyMOL software. Multiple sequences and pair-wise sequence alignments were generated by Clustal Omega (Sievers et al., 2011) and EMBOSS needle tools (Li et al., 2015), respectively. The phylogenetic tree was constructed using the neighbor-joining method available in MEGA7 software with 5000 bootstraps to investigate the relationship between HaGrx1 with other Grx1 orthologs (Kumar et al., 2016).

2.2.3. Sample collection for tissue-specific distribution and temporal expression analysis

Sample collection for both tissue distribution and the temporal expression was carried out as described previously (Oh et al., 2016). Healthy big-belly seahorses were acquired from the Korea Marine Ornamental Fish Breeding Center (Jeju Island, Republic of Korea) and kept in 300 L tanks with temperature of $18 \pm 2^\circ\text{C}$ and practical salinity units (psu) of 34 ± 0.6 for one week. Then, six healthy big-belly seahorses (three males and three females with an average body weight of 8 g) were dissected, and 14 tissues including liver, testis, ovary, spleen, intestine, gill, kidney, skin, muscle, heart, pouch, stomach and brain were carefully isolated for tissue-specific transcriptional analysis. Blood was collected by tail cutting, and the peripheral blood cells were separated by centrifugation at $3000 \times g$ for 10 min at 4°C . Then, all tissues were immediately snap frozen in liquid nitrogen and stored at -80°C .

For the temporal expression analysis experiment, big-belly seahorses were divided into five groups, and each group contained 35 juvenile big-belly seahorses having an average body weight of 3 g. Each group was intraperitoneally injected with 100 μL of lipopolysaccharides (LPS) (1.25 $\mu\text{g}/\mu\text{L}$), polyinosinic:polycytidylic acid (poly I:C) (1.5 $\mu\text{g}/\mu\text{L}$), *Edwardsiella tarda* (5×10^3 CFU/ μL), and *Streptococcus iniae* (1×10^5 CFU/ μL), which were suspended phosphate buffered saline (PBS). The control group was injected with 100 μL of PBS. Next, blood was collected from five seahorses at 3, 6, 12, 24, 48, and 72 h post-injection (p.i.) intervals. During the temporal expression analysis

experiment period, seahorses were not fed. All experiments in this study including seahorse rearing and temporal expression were reviewed and approved by the Animal Care and Use Committee of Jeju National University.

2.2.4. RNA extraction and cDNA synthesis

Total RNA was extracted from a pool of excised tissues (tissue distribution $n = 6$ and temporal expression $n = 5$) using RNAiso plus reagent (TaKaRa, Japan) and cleaned up with RNeasy spin column (Qiagen, USA) according to the manufacturer's protocol. The quality of the extracted RNA was assessed by 1.5% agarose gel, and the concentration was recorded at 260 nm using a μ Drop Plate (Thermo Scientific, USA). Then, 2.5 μ g of total RNA was reverse transcribed using the PrimeScript™ II 1st Strand cDNA synthesis kit (TaKaRa, Japan). Finally, synthesized cDNA was diluted 40-fold in nuclease-free water and stored at -80°C .

2.2.5. Quantitative real-time PCR (qPCR) analysis

Tissue-specific and temporal mRNA expression of *HaGrx1* were measured by qPCR using TaKaRa Thermal Cycler Dice Real Time System III. All qPCR primers were designed according to the minimum information for publication of quantitative real-time PCR experiments (MIQE) guidelines (Bustin et al., 2009) using the IDT primer quest tool (<https://sg.idtdna.com>). Big-belly seahorse 40S ribosomal protein S7 gene (Accession No: KP780177) was selected as an internal control gene. The qPCR reaction was performed in a total 10 μ L reaction mixture composed of 3 μ L of cDNA template, 5 μ L of TaKaRa Ex Taq™ SYBR premix (TaKaRa, Japan), 1.2 μ L of PCR grade water, and 0.4 μ L of each primer (10 pmol/ μ L) as cited in Table 01. Initial denaturation, denaturation, annealing, and extension parameters for a qPCR cycle were 10 s at 95°C , 5 s at 95°C , 10 s at 58°C , and 20 s at 72°C , respectively. After 45 cycles, a final cycle of 15 s at 95°C , 30 s at 60°C , and 15 s at 95°C was run to evaluate the specificity of target amplification.

2.2.6. Statistical analyses of qPCR data

Relative mRNA expression of *HaGrx1* was calculated by the Livak ($2^{-\Delta\Delta CT}$) method (Livak and Schmittgen, 2001). For tissue-specific expression data analysis, the Ct value of skin tissue was set as the basal expression. Relative *HaGrx1* expression values were statistically analyzed by one-way ANOVA using IBM SPSS 24 software (SPSS, USA). For the immune challenge expression analysis, mRNA expressions at different p.i. intervals were represented as fold changes relative to the PBS and unchallenged controls at each time point. Fold values were further statistically compared ($p < 0.05$) with un-injected control (0 p.i) by the Mann-Whitney *U* test using the IBM SPSS 24 software. All determinations were carried out in triplicates, and the results are expressed as the mean \pm standard deviation (SD).

2.2.7. Recombinant plasmid construction

Specific cloning primers with corresponding restrictions sites were designed for recombinant plasmid construction (Table 1). The *HaGrx1* coding sequence was amplified by PCR using template cDNA derived from blood. The total volume of 50 μ L of PCR reaction mixture was prepared by adding 0.4 μ L of Ex Taq polymerase (5 U/ μ L, TaKaRa, Japan), 2 μ L (10 pmol/ μ L) of respective forward and reverse primers, 5 μ L of 10 \times ExTaq buffer, 4 μ L of 2.5 mM dNTP, and 10 μ L of 40-fold diluted cDNA. The PCR conditions were as follows: an initial denaturation at 94°C for 4 min, followed by 35 cycles at 94°C for 30 s, 56°C for 30 s, 72°C for 70 s, and a final extension at 72°C for 10 min. Then, the PCR product was purified by the Accuprep® PCR purification kit (Bioneer Co., Korea). Amplified PCR products and the pMAL c5x vectors (New England BioLabs Inc.) were subjected to restriction digestion with respective restriction enzymes according to the manufacturer's instructions (TaKaRa, Japan). Next, PCR fragments and the pMAL c5x vectors were subjected to gel electrophoresis and purified by the Accuprep® Gel purification kit (Bioneer Co., Korea). Digested pMAL c5x vector and *HaGrx1* fragments were ligated by Ligation Mighty Mix (TaKaRa, Japan) for 30 min at 16°C. Then, recombinant vectors were transformed into *Escherichia coli* (DH5 α) competent cells by the heat-shock method and positive clones were isolated by the

Accuprep® Plasmid Mini Extraction kit (Bioneer Co., Korea). Finally, the sequence of recombinant HaGrx1 (rHaGrx1) was confirmed by sequencing (Macrogen, Korea).

Table 1: Primers used for cloning and quantitative real-time PCR.

Primer Name	Sequence 5' - 3'	Description
HaGrx1 qPCR forward	GCGCGTCAAGACATGAATAG	T _m 61 °C, 139 bp
HaGrx1 qPCR reverse	CCAGTTTGCCACTCTTATGC	T _m 60 °C, 139 bp
HaGrx1 cloning forward	GAGAGAgatatacATGGCTCAGCAATTCGTCCAGGCTAAAA	T _m 59.9 °C, 436 bp, EcoRV
HaGrx1 cloning reverse	GAGAGAgaattcTCACTGGAGAACCCCAATGGACT	T _m 60 °C, 436 bp, EcoRI
40S ribosomal S7 forward	ACTCTGGAAGTGGCAGAGGAAGAC	T _m 60 °C, 187 bp
40S ribosomal S7 reverse	TGAAGTCATTCATGTTGGTGGCCTGTA	T _m 60 °C, 187 bp

2.2.8. Overexpression and purification of HaGrx1 fusion protein

The recombinant plasmids with verified sequences were transformed into *E. coli* BL21 (DE3) competent cells and cultured in Luria-Bertani (LB) rich ampicillin medium (LB+ 0.2% glucose, 100 µg/mL of ampicillin). Cells were incubated at 37°C at 200 rpm until growth reached an optical density at 600 nm (OD₆₀₀) of 0.5. Then, rHaGrx1 protein expression was induced by adding 1 mM isopropyl β-D-1-thiogalactopyranoside (IPTG) solution and further incubated at 25°C and 200 rpm for 8 h. At the end of the incubation process, cells were harvested by centrifugation at 3000 × g for 30 min at 4°C. The pellet was resuspended in 25 mL column buffer (20 mM Tris-HCl pH 7.4 and 200 mM NaCl) and stored at -20°C for overnight. Cold resuspensions were thawed and lysed by cold sonication. Then, the rHaGrx1 protein was purified as a fusion protein of maltose binding protein (MBP) by pMAL protein fusion and purification systems (NEB, USA) according to the manufacturer's instructions. MBP tag was then cleaved off with factor Xa digestion. The concentration of protein was recorded at OD₅₉₅ by the Bradford method using bovine serum albumin (BSA) as a standard. Protein banding pattern at different steps of purification was visualized by 12% sodium dodecyl sulfate-polyacrylamide gel electrophoresis (SDS-PAGE).

2.2.9. Functional assays

2.2.9.1. Dehydroascorbic (DHA) reductase assay

The DHA reductase activity of rHaGrx1 was assayed by the direct spectrophotometric method mentioned by Wells *et al.* and Stahl *et al.* (Stahl *et al.*, 1983; Wells *et al.*, 1990). Briefly, a series of 200 μ L of a reaction mixture containing 200 mM sodium phosphate buffer (pH 6.9), 1 mM EDTA, 2 mM reduced L-Glutathione (GSH) (Sigma, USA), and 25 μ g/mL of rHaGrx1 was prepared in order to perform kinetic analysis for rHaGrx1 with respect to DHA concentration. The reaction was initiated by adding a series of DHA solutions with varying concentrations (0, 0.5, 1, 1.5, and 2 mM) (Sigma, USA). Initial and final absorbance was measured at 265 nm with 2-min intervals. rHaGrx1 kinetic activity with respect to GSH concentration was measured using 25 μ g/mL of rHaGrx1, 1.5 mM DHA, and a series of GSH solutions with varying concentrations (0, 0.5, 1, 1.5 and 2 mM). A blank without protein was simultaneously run for each reaction in order to eliminate background error occurred by any nonenzymic reaction between GSH and DHA. All spectrophotometric data were obtained by the SYNERGY/HT™ microplate reader (Biotek, Korea). The experiment was performed in triplicate at 25°C. The Michaelis-Menten constant (K_m) and turnover number (K_{cat}) were determined using the Lineweaver-Burk plot (Silverman, 2000).

2.2.9.2. Relative DHAR activity of HaGrx1 with different thiol compounds

The impact of different thiol compounds on Grx1 activity was measured as described previously with slight modifications (Sa *et al.*, 1997). Reduced GSH, 1,4-dithiothreitol (DTT), L-cysteine, and 2-mercaptoethanol (all from Sigma-Aldrich, USA) were used as thiol compounds. The dehydroascorbic reduction assay was performed as described in section 3.4.1 using 12.5 μ g/mL rHaGrx1 protein, 0.5 mM DHA and 2 mM thiol compound. The HaGrx1 activity in the presence of the different thiol compounds was calculated relative to HaGrx1 activity with GSH as 100%. Relative HaGrx1 activities were statistically compared ($p < 0.05$) using Kruskal–Wallis one-way analysis of variance test using IBM SPSS 24 software.

2.2.9.3. β -Hydroxyethyl Disulfide (HED) and reduction assay

HED reduction activity of rHaGrx1 was assayed as described previously by measuring the decrease in absorbance at 340 nm [37,38]. For the kinetic analysis of GSH, the reaction was performed in a 500 μ L reaction mixture containing 100 mM Tris-HCl (pH 7.9), 0.2 mM NADPH, 2 mM EDTA, 0.1 mg/mL bovine serum albumin, 0.1 μ g/mL glutathione reductase, 0.7 mM HED, and different GSH concentrations (0.2-2 mM). After adding HED, the absorbance was measured for 3 min (30-sec intervals) in order to confirm the termination of the nonenzymic spontaneous reaction between HED and GSH. Then, 0.19 μ M rHaGrx1 was added to initiate the enzymatic reaction, and the absorbance at 340 nm was recorded for 2 min. Similarly, kinetic analyses for HED were determined using varying concentrations of HED (0.3-1.8 mM) in the presence of 1 mM GSH and 0.19 μ M rHaGrx1. K_m and K_{cat} values were calculated by the Lineweaver-Burk plot method.

2.2.9.4. Turbidimetric assay of insulin disulfide reduction

The rate of insulin disulfide reduction by rHaGrx1 was monitored spectrophotometrically at 650 nm as described previously (Zaffagnini et al., 2008). The 200 μ L reaction mixture contained 0.1 M potassium phosphate buffer (pH 7.9), 0.13 mM bovine insulin, 2 mM EDTA, and different concentrations of rHaGrx1 (2-17 mM). The reaction was initiated by adding 1 mM GSH as a reductant. The treatments were statistically compared ($p < 0.05$) with 0 μ g/mL protein + GSH control by independent Student's t-test using IBM SPSS statistics 24 software.

2.3. Results

2.3.1. Sequence analysis of HaGrx1

The length of the coding sequence of HaGrx1 (Accession No. MK078310) was 321 bp and encoded a protein with 106 amino acids (aa). The theoretical isoelectric point (pI) and molecular mass of the deduced HaGrx1 protein were 7.71 and 11.77 kDa, respectively. HaGrx1 does not contain any signal peptides or N-linked glycosylation sites. According to the NCBI conserved domain database, HaGrx1 consists of a glutaredoxin conserved domain (14-98 aa) and belongs to

the thioredoxin-like superfamily. Further, it contains a CSYC (23-26 aa) active site which represents the conserved CXXC thioredoxin/glutaredoxin catalytic motif. Moreover, HaGrx1 has 11 GSH binding sites as depicted in Figure 1.

CCCCTTCGTCGTCCACCTCAAACCTCAAG

```

0  ATG GCT CAG CAA TTC GTC CAG GCT AAA ATC AAA GGA GAC AAA GTG GTT TTG  51
0  M  A  Q  Q  F  V  Q  A  K  I  K  G  D  K  V  V  L  17
52  TTC ATT AAG CCC ACA TGC TCG TAC TGT GTC ACT GCC AGG GAA GTT CTA TTG  103
18  F  I  K  P  T  C  S  Y  C  V  T  A  R  E  V  L  L  34
104  AAG TAC AAA TTC AAG CCG GGA CAT CTG GAA TTT GTT GAC ATC AGC GCG CGT  155
35  K  Y  K  F  K  P  G  H  L  E  F  V  D  I  S  A  R  51
156  CAA GAC ATG AAT AGC TTG CAG GAT TAC TTC ATG GAA CTC ACC GGG GCC CGC  207
52  Q  D  M  N  S  L  Q  D  Y  F  M  E  L  T  G  A  R  68
208  ACA GTC CCT CGG GTG TTC ATC GGA GAG GAG TGT GTC GGT GGT GGC AGT GAT  259
69  T  V  P  R  V  F  I  G  E  E  C  V  G  G  G  S  D  85
260  GTG GCA GAG CTG CAT AAG AGT GGC AAA CTG GAG GGA ATG TTG CAG TCC ATT  311
86  V  A  E  L  H  K  S  G  K  L  E  G  M  L  Q  S  I  102
312  GGG GTT CTC CAG TGA  327
103  G  V  L  Q  *  107

CTTAAACTATCAGGTAGGGTACTGAAAGAGTTGAATCGATTTTTACAAACAAGCGAAAGAAATACAC
AAGATGCTGTGAATCCGCTCTTTGTTGTCGATTACTCACGTTGTCCAGGTAGGCGTTGCTTTGTCA
AATGTGCATGAAGAGGCACTTGTGTGCTAACAGGTTGGGCAAAAAGTTGTACTCCAATCCACAGGGA
GAAATCGATCACCCAAATGGGTGATGTTTGTAGAAGAAGAGGATGGAAAAACACACGCGCACCATTCTG
AATGTTATGCTATTTGTTCCATCCGCATCGGTCTCGTAAGGGTCTGCGTGTGAGCTGGAGCCTCTCCC
AGGACTGGTCAGCAACCGTTTATTTTACTGCTGATATGTAGTGTAGTTGTCTGCTTTCAACTGTA
ATGCTTTCACTTGGCTCTTTCAATGCACAGCAAATATGTGTTAATCAAGAATGATCATTAAAGCTTT
TATGAAAATCATCAGTGTG

```

Figure 1: Nucleotide and deduced amino acid sequence of HaGrx1 from *Hippocampus abdominalis*. Predicted glutaredoxin domain is shaded in gray, and the conserved CXXC motif is marked with underlined bold red letters. The GSH binding sites of the protein sequence are indicated in bold black letters. The stop signal of the protein is denoted by an asterisk.

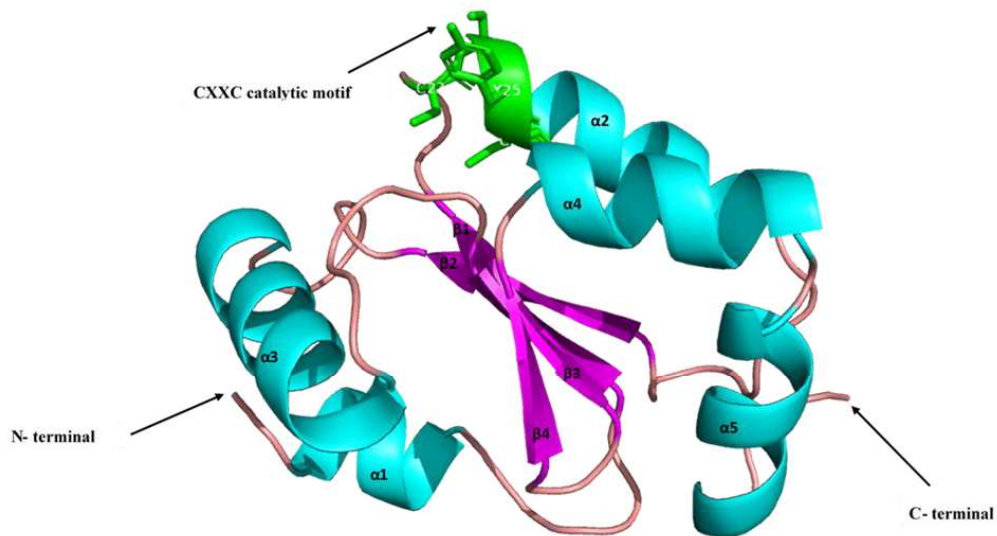


Figure 2: Predicted tertiary structure of *HaGrx1*.

The predicted glutaredoxin domain is shaded in gray, and the conserved CXXC motif is marked with underlined bold red letters. The GSH binding sites of the protein sequence are indicated in bold black letters. The stop signal of the protein is denoted by an asterisk.

The predicted tertiary model for *HaGrx1* covers 77% of the protein's 3D structure (Figure 2). Further, it showed a typical Grx tertiary structure with five α -helices and four β -sheets. According to the multiple sequence alignment (Figure 3A), an active CXXC motif was conserved for all selected *Grx1* orthologs. Further, many of the GSH binding sites that can be found in *HaGrx1* were conserved in other *Grx1* orthologs.

The deduced *HaGrx1* shares the highest identity (97.2%) with *Grx1* homologs of *Hippocampus comes* followed by *Labrus bergylta* (Table 2). Further, *HaGrx1* shared 57.5% sequence identity and 72.6% similarity with the *Grx1* homolog from *Homo sapiens*. According to the phylogenetic reconstruction (Figure 3B), glutaredoxins are universally distributed in all the living organisms including bacteria, plants, and animals. *HaGrx1* was in a clade with other fish *Grx1* counterparts while tightly clustered with the *H. comes* *Grx1* ortholog (Figure 3B).

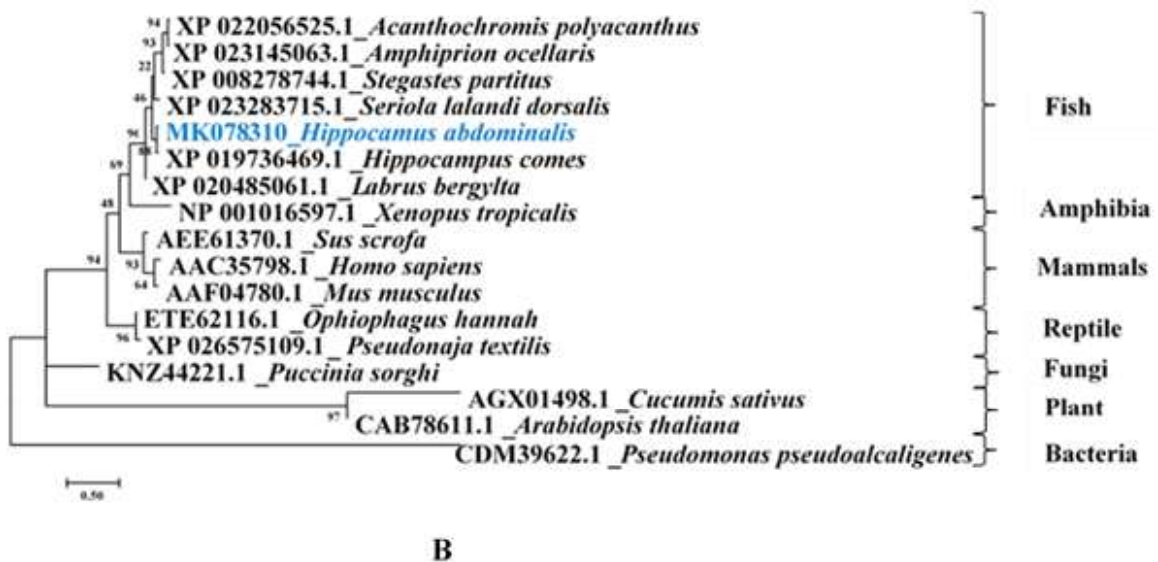
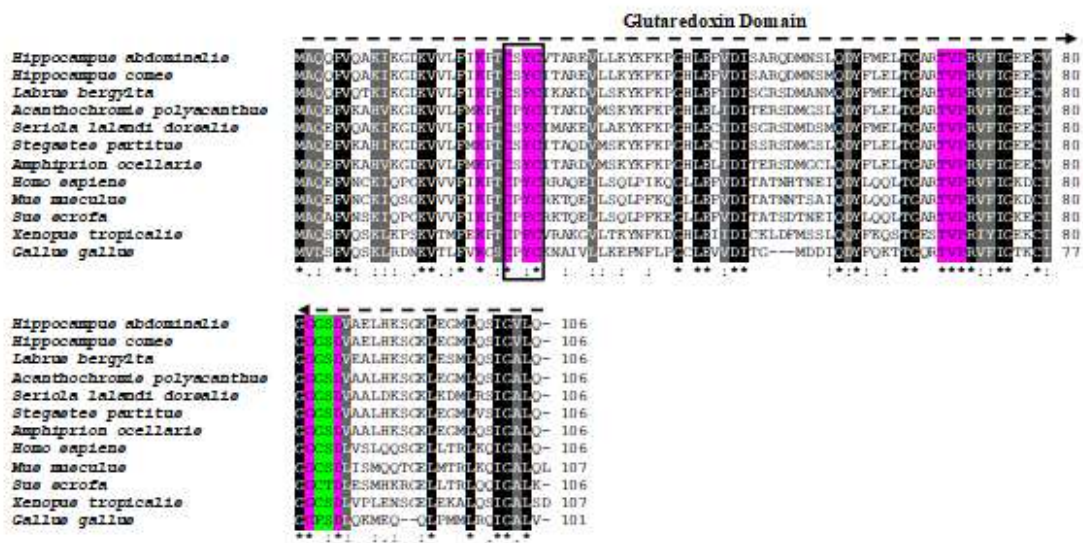


Figure 3: (A) multiple sequence alignment and (B) phylogenetic reconstruction of HaGrx1. Sequence alignments were obtained using the Clustal Omega tool. Conserved residues are shaded in black, and semi-conserved residues are shaded in gray. The conserved CXXC motif is marked with a black box, and GSH binding sites that are conserved in HaGrx1 and all other selected organism are shaded with a purple color. GSH binding sites that are conserved only in selected fish species are marked with green color. Accession numbers of selected protein sequences are listed in Table 2. The evolutionary development of HaGrx1 was analyzed with its different homologs categorized under different taxonomic groups based on the multiple alignment profiles of the protein sequences generated by the Maximum likelihood method using MEGA 7.0 software. Bootstrap support values corresponding to each branch are indicated.

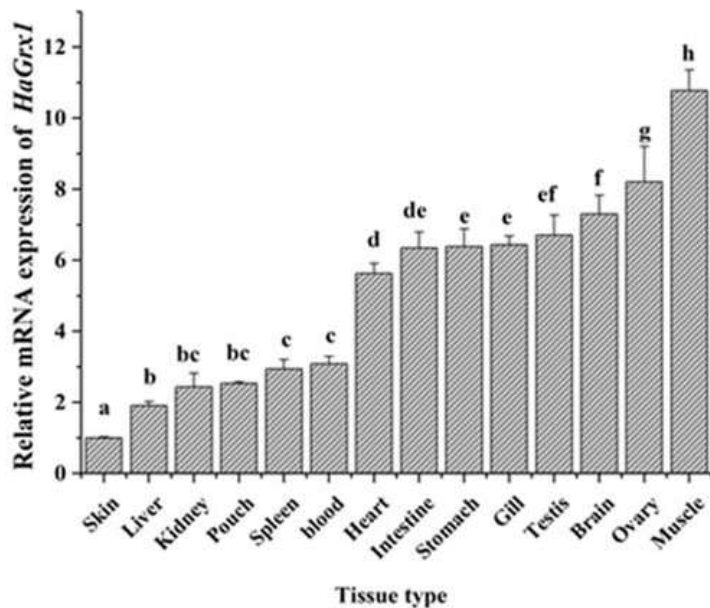
Table 2: Identity and similarity percentages of *Grx1* orthologs from different species compared to *HaGrx1*

Accession No	Scientific name	Identity (%)	Similarity (%)
XP_019736469.1	<i>Hippocampus comes</i>	97.2	100.0
XP_020485061.1	<i>Labrus bergylta</i>	84.0	90.6
XP_023283715.1	<i>Seriola lalandi dorsalis</i>	83.0	91.5
XP_008278744.1	<i>Stegastes partitus</i>	82.1	92.5
XP_023145063.	<i>Amphiprion ocellaris</i>	82.1	91.5
XP_020485061.1	<i>Acanthochromis polyacanthus</i>	81.1	91.5
AAC35798.1	<i>Homo sapiens</i>	57.5	72.6
AEE61370.1	<i>Sus scrofa</i>	57.5	73.6
NP_001016597.1	<i>Xenopus tropicalis</i>	57.0	70.1
AAF04780.1	<i>Mus musculus</i>	54.2	73.8
CAA70437.1	<i>Gallus gallus</i>	47.2	67.0

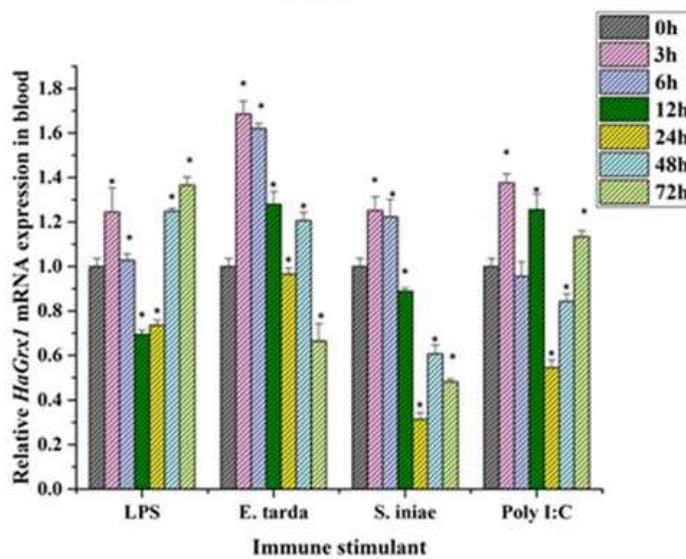
2.3.2. Tissue distribution and immune challenge

As depicted in Figure 4A, *HaGrx1* was ubiquitously expressed in all the 14 tissues tested. The highest expression of *HaGrx1* was observed in muscle, followed by the ovary, whereas the lowest expression was observed in the skin.

According to the temporal expression in the blood (Figure 4B), significant modulations of *HaGrx1* were observed upon treatment with selected PAMPs and live bacteria. *HaGrx1* was significantly upregulated early as 3 h p.i. against LPS challenge, and the significant upregulation was observed at 72 h p.i. *HaGrx1* transcription in response to *E. tarda* showed the highest expression at 3 h p.i. and upregulation lasted for 48 h p.i. *HaGrx1* expression against *S. iniae* showed early upregulation at 3-6 h p.i. For poly I:C, significant *HaGrx1* expression was observed at 3, 12, and 72 h p.i.



A



B

Figure 4: (A) Tissue-specific expression of *HaGrx1* and (B) Temporal expression profiles of *HaGrx1* in the blood after immune stimulation.

The Livak method was used to calculate the relative mRNA expression of each tissue, and seahorse 40S ribosomal protein S7 gene was used as an internal control gene in the qPCR experiment. The data are represented as mean values ($n = 3$) \pm standard deviation (S.D.). For the immune challenge, PAMP (LPS and poly I:C) and bacterial (*Edwardsiella tarda* and *Streptococcus iniae*) were used. The Livak method was used to calculate the fold changes in mRNA expression, and seahorse 40S ribosomal protein S7 gene was used as an internal control gene in the qPCR experiment. The relative fold changes in expression were compared with those of the PBS-injected control at different time points. The data are represented as mean values ($n = 3$) \pm S.D. Significant differences compared to the blank (0 h) are indicated with an asterisk for $P < 0.05$

2.3.3. Expression and purification of rHaGrx1

According to the SDS PAGE gel image (Figure 5), rHaGrx1 can be identified as a single band between 50 kDa and 70 kDa. The approximate size of the predicted band is 54 kDa which represents the rHaGrx1-MBP fusion protein, thus confirming the predicted molecular weight of 11.77 kDa of rHaGrx1.

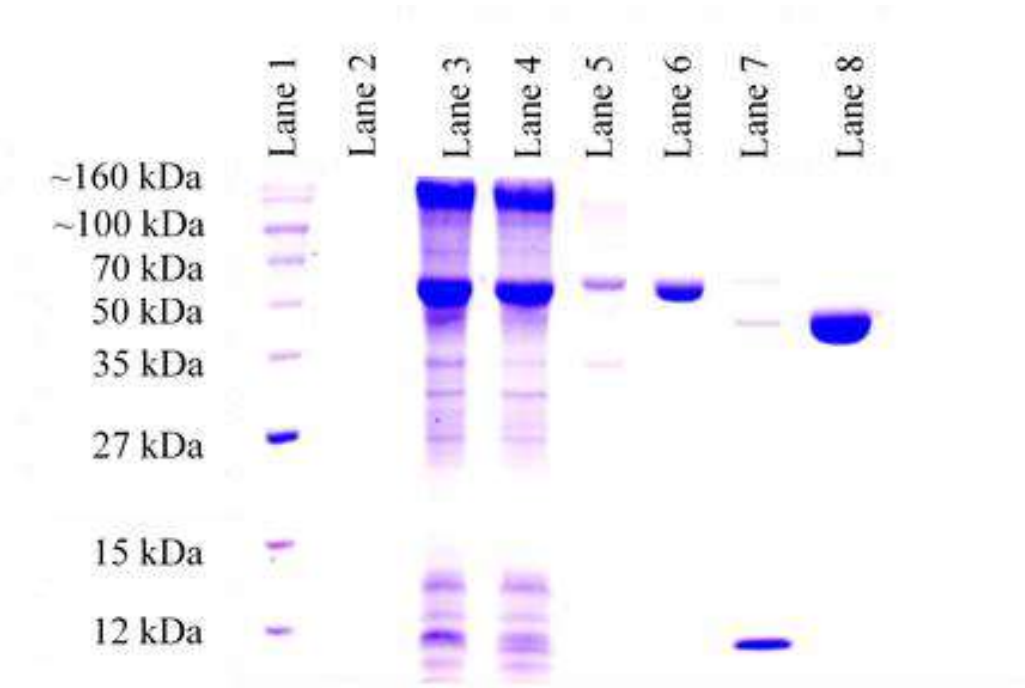


Figure 5: SDS-PAGE figure of rHaGrx1

The SDS-PAGE analysis of overexpressed and purified HaGrx1 as an MBP-fusion protein. Lane 1: unstained protein ladder, Lane 2: crude extract of uninduced *E. coli* C2327 cells, Lane 3: crude extract of induced *E. coli* C2327, Lane 4: supernatant after sonication and centrifugation of induced *E. coli* C2327 cells, Lane 5: Pellet, Lane 6: purified HaGrx1 fusion protein, Lane 7: cleaved rHaGrx1 by factor Xa, Lane 8: Purified MBP protein.

2.3.4. Functional studies

2.3.4.1. Dehydroascorbic (DHA) reduction assay

Table 3: Kinetic parameters of rHaGrx1 for DHA and HED assays at 25 °C. The experiment was conducted in triplicates and data represent mean \pm SD

Substrates	DHA assay		HED assay	
	GSH	DHA	GSH	HED
K_m (mM)	1.56 \pm 0.132	0.57 \pm 0.154	3.21 \pm 0.875	0.21 \pm 0.032
K_{cat} (s⁻¹)	4.86 \pm 0.186	4.62 \pm 0.321	18.3 \pm 0.86	48.8 \pm 1.72
K_{cat/km} (M⁻¹s⁻¹)	3.11 \times 10 ³	8.105 \times 10 ³	5.7 \times 10 ³	2.32 \times 10 ⁵

The dehydroascorbic reduction activity of rHaGrx1 was analyzed using 25 μ g/mL protein. The rHaGrx1 showed significant DHA reduction activity compared to the control. As seen in Figure 6A, the DHA reduction activity of rHaGrx1 increased linearly up to 2 min with 0.5-2 mM DHA concentrations at constant GSH concentration. The DHA reduction activity of rHaGrx1 increased linearly up to 2 min with 0.5-2.0 mM GSH at constant DHA concentrations (Figure 6B). Kinetic analysis of the DHA reduction activity of rHaGrx1 revealed apparent K_m and K_{cat} values with respect to each substrate that is shown in Table 3.

2.3.4.2. Relative DHAR activity of HaGrx1 with different thiol compounds

Since various thiol compounds may activate the Grx, the DHAR activity of rHaGrx1 was determined using four reducing thiol compounds. HaGrx1 showed the highest DHAR activity in the presence of DTT as the reductant thiol compound (Figure 6C). The DHAR activity of HaGrx1 differed in order of DTT > GSH > 2-ME > L-cysteine with the thiol compounds.

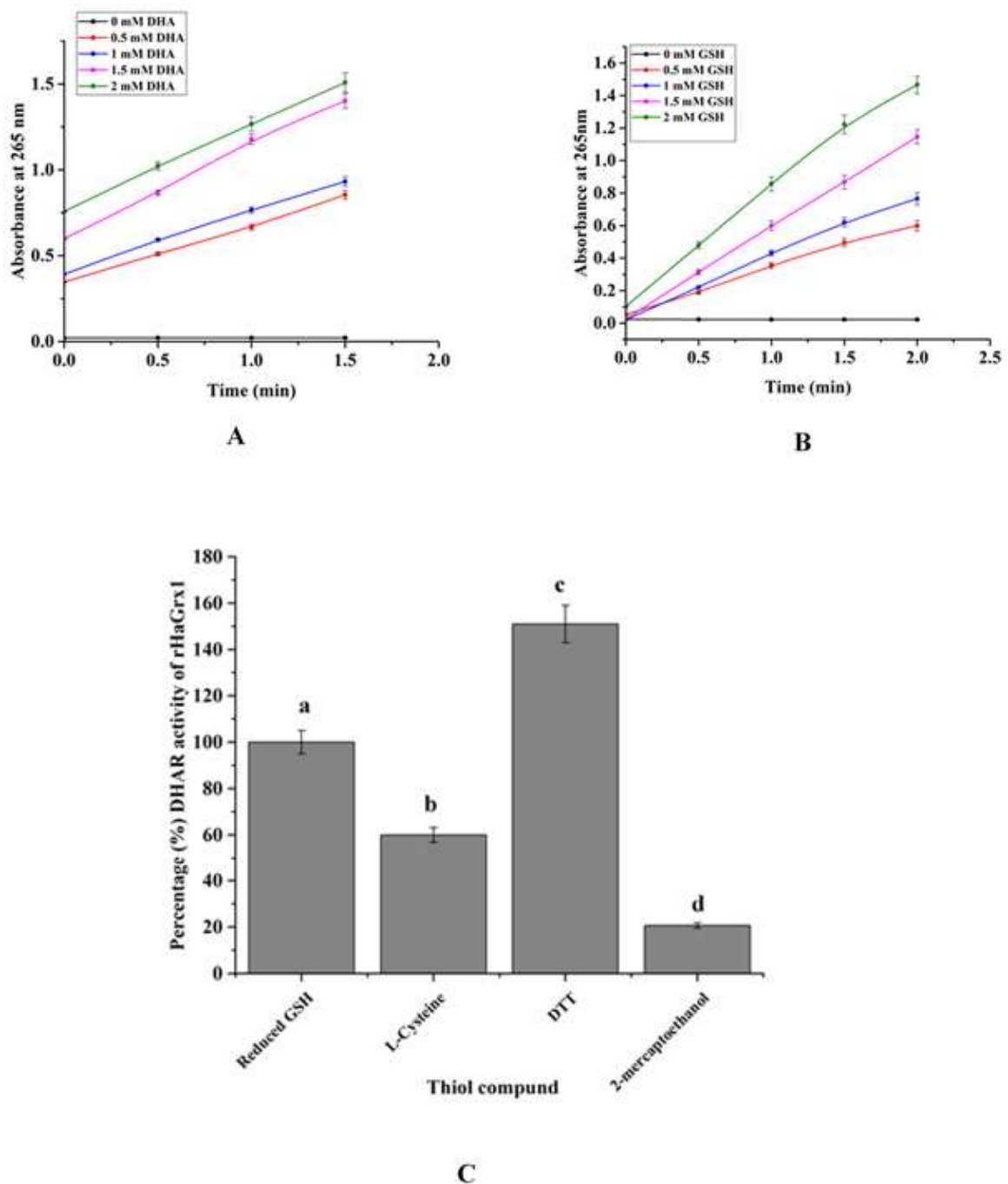


Figure 6: (A) DHA reduction activity of *rHaGrx1* with different DHA concentration and (B) with different GSH concentration

The data are represented as mean values ($n = 3$) \pm SD. (C) Dehydroascorbate reductase activity of *rHaGrx1* with different reducing thiol compounds at 25°C. The experiment was conducted in triplicates. The data represent the percentage (mean \pm SD). Data with different letters are significantly different among each group ($p < 0.05$).

2.3.4.3. HED reduction assay

The small molecular weight disulfide reduction activity of rHaGrx1 was analyzed by HED assay. rHaGrx1 showed significant disulfide reduction activity with different GSH concentrations. HED reduction activity of rHaGrx1 was increased in a GSH concentration-dependent manner at a constant HED concentration (Figure 7). The apparent K_m , and K_{cat} with respect to GSH were cited in Table 3.

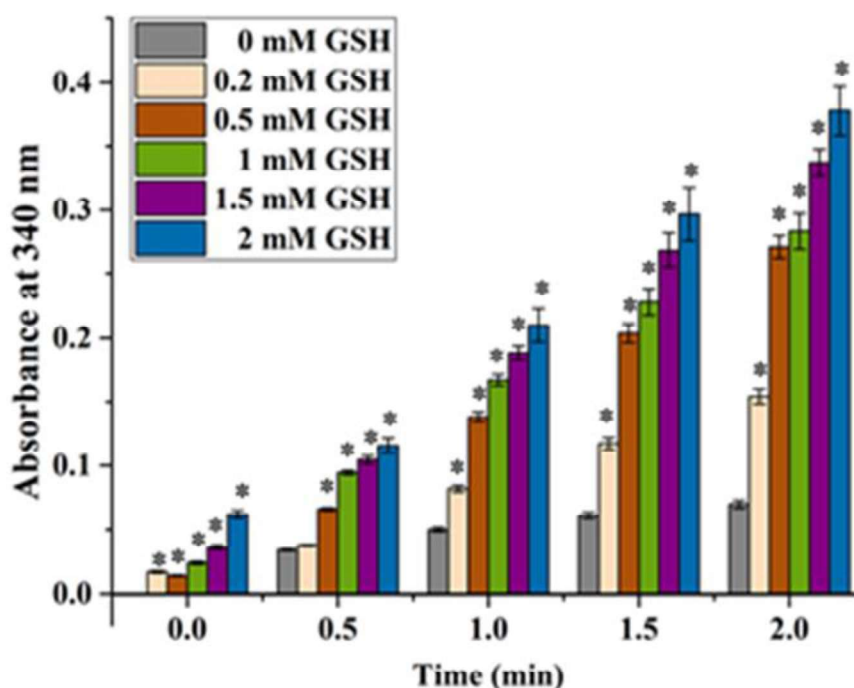


Figure 7: HED reduction activity of rHaGrx1 with different GSH concentrations at 25°C. Data obtained from triplicate determinations and are expressed as mean values \pm SD. Significant differences compared to 0 mM GSH are indicated with “*” ($p < 0.05$).

2.3.4.4. Turbidimetric assay of insulin disulfide reduction

Insulin disulfide reduction assay was performed to evaluate the oxidoreductase activity of rHaGrx1. According to data shown in Figure 08, significant insulin reduction activity was observed upon 5 min in GSH + rHaGrx1 treated samples. Higher insulin reduction activity was observed in the 200 μ g/mL rHaGrx1 + GSH sample compared to lower concentrations of rHaGrx1 + GSH. However, disulfide reduction activity was not detected within the observed incubation period for

rHaGrx1 in the absence of GSH. Further, samples containing only GSH showed lower absorbance compared to those of the rHaGrx1 + GSH treated samples.

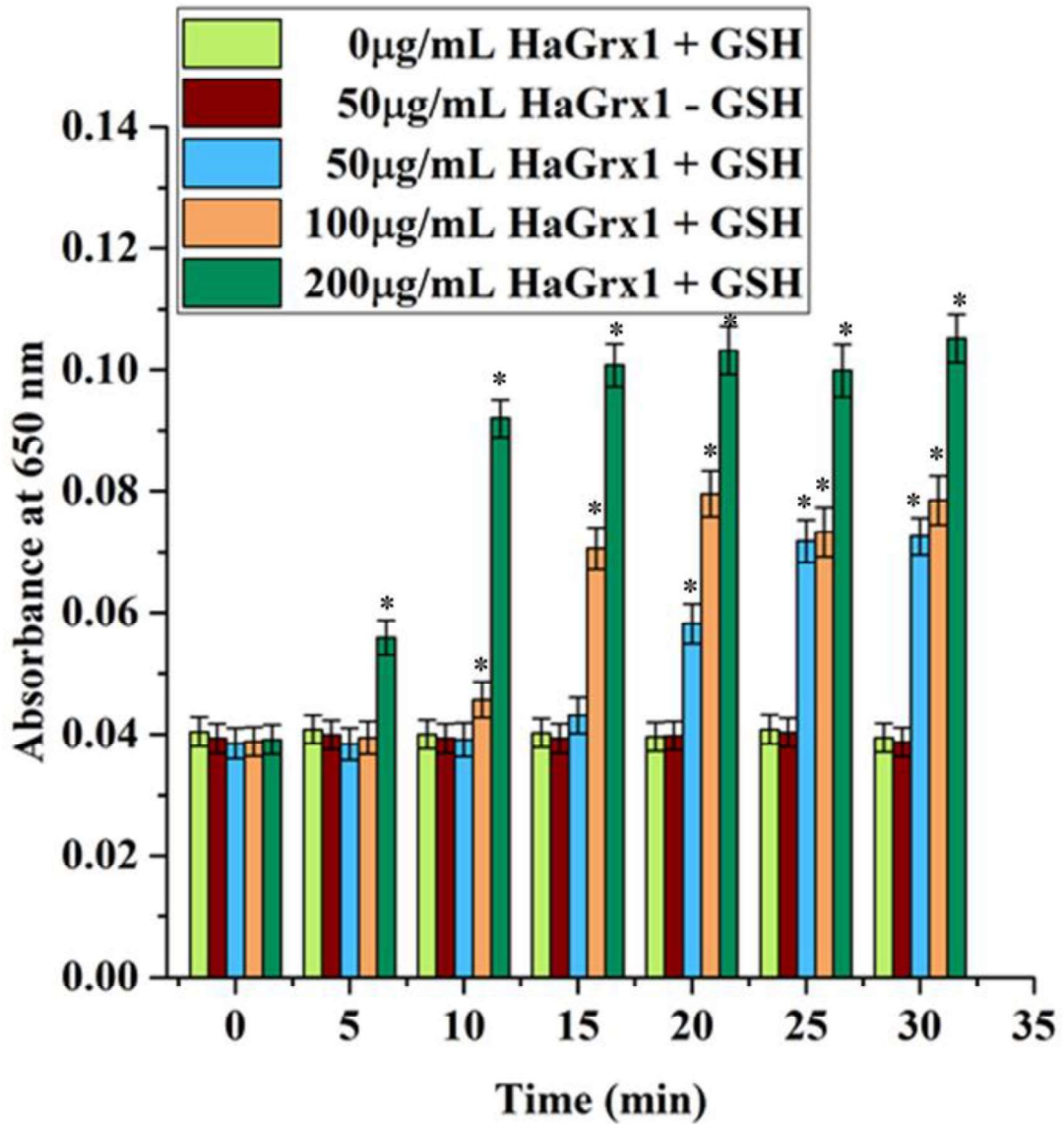


Figure 8: Insulin disulfide reduction activity of rHaGrx1 with different protein and GSH combinations.

The turbidity was measured every 5 min incubation at 25°C at 650 nm. Data were obtained from triplicate determinations and are expressed as mean values \pm SD. Significant differences ($p < 0.05$) compared to control (0 μ g/mL rHaGrx1+GSH) are indicated by *.

2.4 Discussion

Redox-active thiol-containing proteins such as Trx and Grx play a vital role in redox homeostasis which leads to scavenging of reactive oxygen species (ROS). ROS accumulation causes various pathological conditions and consequently leads to cell damage and apoptosis (Ray et al., 2012). There are many studies on Grx1 orthologs from different species including viruses (Davis et al., 1997), bacteria (Vlamis-Gardikas et al., 1997), fungi (Herrero et al., 2006), plants (La Camera et al., 2011), and mammals (Terada et al., 1992), but few functional studies from fish species regarding innate immunity and oxidative stress. In this study, characteristics of HaGrx1 were evaluated based on *in-silico* analysis, innate immune responses, and redox activity.

The deduced HaGrx1 protein sequence possessed similar characteristics to those of Grx1 from other species. For example, human Grx1 showed identical features to HaGrx1 (Fernando et al., 1994). Further, the molecular mass of human Grx1 and HaGrx1 is 11.76 and 11.77 kDa, respectively. *E. coli* Grx also has similar features such as a molecular weight of 10 kDa and a CXXC active site (Fernandes and Holmgren, 2004). Therefore, the structure of Grxs appeared to be conserved to both eukaryotes and prokaryotes. HaGrx1 has 11 GSH binding sites that are essential for its function. Usually, GSH acts as an electron donor for many proteins such as Grx, Glutathione S-transferase (GST), and Glutathione reductase (GR). Therefore, GSH binding sites are essential for the redox function of such proteins. Among the 11 GSH binding sites in HaGrx1, nine residues are highly conserved in vertebrates, whereas all 11 residues are conserved and represented by the same amino acid in fish Grx1 orthologs (Figure 3A). Hence, HaGrx1 may be classified as a glutaredoxin with typical sequence characteristics. However, the CXXC catalytic motif is commonly represented as CPYC in other species, but HaGrx1 contains CSYC residues, which can also be observed in some fish species (Figure 3A). According to Foloppe *et al.*, redox activity of the CXXC motif in *E. coli* can be significantly affected by alterations in -X-X- residues (Foloppe and Nilsson, 2004). Therefore, alteration of CPYC to CSYC can change the redox properties of the HaGrx1 sequence. This point can be further emphasized by the fact that human Grx2, which contains CSYC, has the ability to obtain electrons from mitochondrial thioredoxin reductase and coordinating Fe/S clusters (Foloppe

and Nilsson, 2004). Further, alterations in peripheral amino acids can significantly affect the redox potential (Foloppe and Nilsson, 2004). Therefore, HaGrx1 may possess different catalytic properties from all other Grx1 orthologs.

The tertiary structure of HaGrx1 showed 77% similarity to human Grx1 PDB template, suggesting that it has a typical Grx1 3D structure. HaGrx1 also has a typical thioredoxin fold, which is conserved in enzymes that catalyze disulfide bond formation and isomerization. The spatial topology of the thioredoxin fold comprises central four antiparallel β -sheets surrounded by three α -helices (Martin, 1995). However, HaGrx1 was found to consist of 5 α -helices. It has been reported that most prokaryotic Grxs contain a typical thioredoxin structure, but some eukaryotic Grxs possess two additional α -helices on the N- and C-termini (Berndt et al., 2008). Due to the conserved structural features, HaGrx1 showed 57.5% identity with human Grx1 amino acid sequence, but according to data shown in Figure 3B and phylogenetic reconstruction, HaGrx1 is more closely related to fish Grx1 orthologs. Moreover, HaGrx1 shows the highest homology with Grx1 from *H. comes*. Therefore, the *in-silico* analysis results in this study provide clear evidence of the evolutionary link and the ancestral lineage of HaGrx1 to other Grx1 orthologs.

The conservation of Grx structure and function throughout all organisms, even plants and viruses, denotes the importance of its functions for biological processes. The most well-elucidated function of Grx1 is its role in regulating redox homeostasis, which has a significant influence on immune, metabolic, and hormonal functions (Hanschmann et al., 2013a). The antioxidant activity of Grx is exerted by an enzymatic system comprised of GSH, glutathione reductase (GR), and NADPH (Berndt et al., 2006). Grx is a key reducing agent present in cells that can catalyze the activity of a versatile range of substrates. By catalyzing these substrates, Grx1 regulates many metabolic and signaling pathways, and thus is recognized as a transcription factor for many genes such as Bcl-2, Bcl-xL, and apurinic (apyrimidinic) endonuclease/redox-factor 1 (APE/Ref-1) (Gallogly et al., 2010).

Further, it is reported that the redox activity of Grx1 can functionally overlap with the activity of many proteins. For instance, it catalyzes many substrates utilized by Trx such as insulin and ribonucleotide reductase (Arnér and Holmgren, 2000). Further, it possesses dehydroascorbic

reductase activity, glutathione peroxidase activity, and glutathione S-transferase activity (Collinson and Grant, 2003; Fernandes and Holmgren, 2004; Wells et al., 1990). Most importantly, Grxs are involved in Fe/S cluster coordination in cells (Bräutigam et al., 2013). Hence, Grx1 can be recognized as a multifunctional enzyme, thereby ubiquitous expression in tissues can be expected. The tissue-specific expression of *HaGrx1* also exhibited ubiquitous expression in all the tissues examined, and the highest significant expression was observed in muscle. ROS are highly generated in muscles due to the high energy production and utilization of this tissue (Powers et al., 2014). Seahorses are tiny sea creatures with characteristic skeletal and muscle structures required for swimming and to anchor to substrates (Woods, 2007). They have a strong prehensile tail that attaches to substrates and a large dorsal fin that exerts propulsive force to swim in an upright position (Woods, 2007). Therefore, muscles attached to fins and the skeleton are highly active, and ROS generation can be increased in this tissue. The highest expression of *HaGrx1* in muscle suggests its requirement for ROS neutralization. The second highest expression was observed in the ovary followed by brain tissue (Figure 4A). Ovaries are metabolically active and undergo various stresses (Sugino, 2005). Fernández *et al.* reported that Grx1 expression in rat ovary significantly influences the maturation of oocytes and survival of luteal cells by protecting them from apoptosis and oxidative damage (González-Fernández et al., 2005). As female seahorses produce more than 1500 eggs/clutch, ovaries are highly active (Vincent, 1996). Therefore, significant *HaGrx1* production in this tissue suggests that it protects eggs from oxidative stress during maturation. Also, Grxs are intensively investigated upon protecting the central nervous system from oxidative stress (Berndt et al., 2014; Daily et al., 2001; Takagi et al., 1999). Further, it is reported that Grx protects cerebellar granule neurons from dopamine-induced apoptosis by activating NF- κ B (Daily et al., 2001). Ascorbic acid is one of the key antioxidant molecules needed for several functions of the central nervous system, including the maturation and differentiation of neurons, myelin formation and synthesis of catecholamine (Wilson and Wilson, 2002). Therefore, significant tissue-specific expression of *HaGrx1* in the brain may be evidence that antioxidant function is required for the recovery of ascorbic as well as the elimination of ROS, which can cause neurodegeneration.

Grxs plays an essential antioxidant role in the blood as red blood cells are highly exposed to xenobiotics and ROS formed during inflammation. Therefore, vertebrate RBCs have their reactive sulfhydryl groups on each β subunit, and they can exert antioxidant activity against free radicals such as H_2O_2 (Richards, 1996; Titrant, 1982). However, oxidation of these SH- groups can affect the oxygen- and heme-binding capacity of the RBCs (Papov et al., 1994). Therefore, it is reported that Grx in erythrocytes has a distinct function in regenerating oxidized SH groups on RBCs (Papov et al., 1994). On the other hand, it is reported that erythrocytes have a bactericidal effect by producing ROS against pathogens (Minasyan, 2014). Thus, it is important to regulate ROS production to a proper level to avoid causing cell damages. As a result, expression of Grx1 in blood during pathogenic infection is essential in many ways. The significant modulation of *HaGrx1* transcripts in blood upon exposure to pathogens such as *E. tarda* and *S. iniae* suggests both sulfhydryl homeostasis and ROS neutralization. In addition, Grx1 can activate IL-1 and TLR-4 signaling pathway by regulating TRAF6 (Chantzoura et al., 2010). IL-1 is a proinflammatory cytokine that promotes the activation of immune cells such as macrophages, monocytes, lymphocytes, and neutrophils (Dinarello, 1997). TLR-4 also acts as a receptor for LPS and regulates the secretion of proinflammatory factors (Lu et al., 2008). Both IL-1 and LPS activate myeloid differentiation factor 88 and TRAF6 and thus promote proinflammatory signaling cascades as an innate immune response (Dinarello, 1997; Lu et al., 2008). TRAF6 is deglutathionylated by Grx1 upon IL-1 induction, and it can activate the NF- κ B pathway (Chantzoura et al., 2010). Further, Grx1 can promote the autopolyubiquitination of TRAF6, which subsequently activates NF- κ B (Chantzoura et al., 2010). These proinflammatory pathways are highly active during immune stimulation. Therefore, significant upregulation of *HaGrx1* in blood upon exposure to LPS, *E. tarda*, and *S. iniae* can indicate the activation of proinflammatory pathways by deglutathionylation of TRAF6. Poly I:C is a synthetic compound analog to viral dsRNA. It can activate IRF3 through the TLR3 signaling cascade. IRF3 is a key transcription regulatory factor of antiviral interferon genes. During viral infections, IRF3 translocates to the nucleus and activate transcription. Deglutathionylation of IRF3 is essential to activate IRF3 and the gene expression of IFN β . Prinarakis *et al.* reported that the deglutathionylation

of IRF3 is regulated by cytoplasmic Grx1 in humans. Therefore, Grx1 plays a crucial role in controlling the cell signaling pathway upon viral infection. The significant upregulation of HaGrx1 against Poly I:C may be evidence of activation of IRF3 by deglutathionylation. The aforementioned proinflammatory signaling pathways are essential for innate and adaptive immunity of higher organisms, including the seahorse. *E. tarda* and *S. iniae* can cause severe infections in a broad range of animals. In this study, *HaGrx1* transcriptional profile against immune stimulants show overall upregulation pattern, but significant downregulations can be observed at time points such as 24h upon all the stimuli. The reason for the downregulations is not clear, but Grx1 can be involved in the dynamic regulation of NF- κ B during the infections and oxidative stress. Reynaert *et al.* suggest that key immune regulatory factor NF- κ B is known as redox sensitive molecule and Grx1 potentially involved in controlling the magnitude of activation of the NF- κ B through Grx1 dependent deglutathionylation of IKK- β . Therefore, Grx1 modulates the extent and timing of activation of NF- κ B signaling. They suggest that modulation of NF- κ B and IKK- β upon oxidative and inflammatory responses is a protective mechanism to avoid irreversible inactivation of IKK- β and to ensure rapid regeneration of enzymatic activity (Reynaert et al., 2006). Therefore, the dynamic upregulations and the down regulations that can be observed in this study might reflect the potential involvement of HaGrx1 in the regulation of NF- κ B signaling cascade through its differential expression patterns. Therefore, present results demonstrate that *HaGrx1* transcription regulates the immune responses in the seahorse.

Ascorbic acid (AA) is a highly required cofactor for many enzymes as involved in the biosynthesis of collagen, creatinine, catecholamine, and peptide hormones (Wilson and Wilson, 2002). Further, they terminate free radical chain reactions by scavenging ROS and reactive nitrogen species (RNS). During the above biological processes, AA can be oxidized into DHA which can be used to regenerate AA again (Stahl et al., 1983). The conversion of DHA to AA is mainly catalyzed by GSH-dependent DHA reductase, but some other enzymes such as thioredoxin reductase, Grx, and GST-omega also possess dehydroascorbate reductase (DHAR) activity (Do et al., 2016; May et al., 1997; Zhou et al., 2012). Similarly, HaGrx1 also demonstrated DHAR activity. As shown in Table

3, the K_m value of DHA is lower than the K_m of GSH. Higher K_m value indicates that a high substrate level is required to reach the V_{max} . As HaGrx1 has 11 GSH binding sites, the K_m for GSH can be increased. According to the literature, HaGrx1 shows a similar K_m value to that of bovine thymus glutaredoxin upon DHA exposure (Wells et al., 1990). Further, K_m values of HaGrx1 for GSH are similar to that of human placental thioltransferase (Wells et al., 1990). The catalytic efficiency (V_{max}/K_m) of HaGrx1 for DHA is higher than that of Grx1 from *Chlamydomonas reinhardtii* (Zaffagnini et al., 2008), indicating that HaGrx1 has better redox properties.

Grxs can utilize thiol compounds other than GSH (Bick et al., 1998; Sa et al., 1997). Therefore, we analyzed the DHAR activity of rHaGrx1 with different thiol compounds. Interestingly, the highest relative DHAR activity of rHaGrx1 was observed with DTT. In a prior study, Grxs showed the best activity with GSH as reductant compound (Vlami-Gardikas and Holmgren, 2002). However, another study reported that Grxs have better activity with DTT in assays, including the insulin reductase assay (Gao et al., 2010). DTT has two SH groups and is considered a strong electron donor or reductant (Carmack and Kelley, 1968). It is commonly used in *in vitro* assays of Trx but is not considered a naturally available compound in cells (Holmgren, 1979). L-cysteine is a sulfur-containing non-essential amino acid, which can act as a reducing agent (Atmaca, 2004). L-cysteine may also act as a disulfide reducing agent, and its activity is lower than GSH (Aldini et al., 2018). Our results mirror these previous observations. β -mercaptoethanol is a reducing agent that is used in several enzymatic assays due to its excellent ability to inhibit oxidation of free sulfhydryl residues. According to our results, β -mercaptoethanol was not a suitable reducing agent for rHaGrx1 upon DHAR activity. The nature of the selective activity of Grxs on different thiol compounds remains unclear.

HED is a synthetic compound used as the standard substrate for Grxs. According to the elucidated mechanistic model, HED initially reacts with GSH nonenzymatically to yield a mixed disulfide between GSH and 2-mercaptoethanol (GSSEtOH) (Begas et al., 2015). Therefore, GSSEtOH is the actual substrate for Grx in the HED assay. The CXXC motif of Grx1 serves as SH-groups (thiol groups) that can attack GSSEtOH during the oxidative half-reaction. Subsequently,

GSSEtOH reduces to 2-mercaptoethanol and produces S-glutathionylated Grx. Glutathionylated Grx is regenerated by an oxidative half-reaction with GSH, producing oxidized glutathione (GSSG). The subsequent reaction between NADPH and GSSG, catalyzed by GR, recovers the GSH, as well as NADPH consumption by GR, providing an indirect method to monitor GRX activity spectrophotometrically (Holmgren, 1985). According to data shown in Table 3, HaGrx1 exhibited lower catalytic properties towards GSH compared to those of other Grx1 orthologs (Gallogly et al., 2008; Wells et al., 1990). Johansson *et al.* reported that replacing the proline in CXXC with serine can reduce the catalytic properties compared to other Grx1s containing CPYC (Johansson et al., 2004). However, they reported that CSYC alteration in Grxs could increase the affinity toward the glutathionylated substrate, clarifying the behavior of HaGrx1 towards HED (Table 3).

Insulin is a two-chain heterodimer protein with two peptide chains. A and B chains of insulin are linked by disulfide bonds. (Weiss et al., 2000). These interchain disulfide bonds can be reduced by proteins such as protein disulfide isomerase (PDI), Trx, and various other proteins (Holmgren, 1979). During the insulin disulfide reduction, free A and B chains are precipitated, and turbidity can be measured at 650 nm (Holmgren, 1979). Though some reports suggest that glutaredoxin is not effective in insulin disulfide reduction, some studies reported that Grx could exhibit lower insulin reduction activity compared to thioredoxin in the presence of GSH as an electron donor (Gao et al., 2010; Zaffagnini et al., 2008). According to data shown in Figure 8, HaGrx1 also showed concentration-dependent insulin disulfide reduction activity. However, HaGrx1 displayed lower absorbance values at 650 nm compared to thioredoxin proteins from *Hippocampus abdominalis* (Liyanage et al., 2018).

In conclusion, the *HaGrx1* gene was identified in this study and subjected to various molecular, transcriptional, and functional analyses. HaGrx1 possesses a typical Grx1 structure with a CSYC thioredoxin motif. Spatial and temporal expression analysis showed that *HaGrx1* was constitutively expressed in all the seahorse tissues examined and significantly upregulated in response to LPS, poly I:C, *S. iniae*, and *E. tarda* immune stimulations. Further, HaGrx1 exhibited reductive activity toward DHA, insulin, and HED. Therefore, HaGrx1 could be actively involved in

suppressing oxidative stress from both abiotic and biotic sources. Altogether, the results in this study provide better knowledge about the role of HaGrx1 in the host defense system.

CHAPTER 2

Glutaredoxin 2 from big belly seahorse (*Hippocampus abdominalis*) and its potential involvement in cellular redox homeostasis and host immune responses

3.1. Introduction

Glutaredoxins (Grxs) are glutathione-dependent oxidoreductases that mainly involved in biological redox reactions. Typical Grxs can be divided into two major groups (monothiol and dithiol) depend on the active motif. Monothiol Grxs contain Cys-X-X-Ser as a catalytic motif and dithiol Grxs share Cys-X-X-Cys catalytic motif similar to thioredoxins (Lillig et al., 2008). The X-X in the active site of thioredoxins can be any other amino acid. However, in dithiol Grxs, it is restricted to CPYC and CSYC in vertebrates (Johansson et al., 2004). Grx1 contain CPYC as the active site, and Grx2 contain CSYC In human and most of the mammals (Fernando et al., 1994; Gladyshev et al., 2001). In contrast, most of the fish Grx1 consisted of CSYC, and Grx2 homologs contain CPYC. In human, alteration of active site amino acids (CPYC to CSYC) reported for considerable variations in redox properties (Foloppe and Nilsson, 2004). For example, alteration of proline to serine in mammalian Grx2 provides the ability to Fe-S cluster assembly and accept an electron from both GSH and Thioredoxin reductase (Foloppe and Nilsson, 2004; Johansson et al., 2004). Moreover, it is reported that Grx2 orthologs capable of withstanding H₂O₂ which inhibit other Grxs (Wu et al., 2010).

Typical Grx structure is similar to thioredoxin structure and represents four β sheets surrounded by 3-5 alpha helixes (Lillig et al., 2008). Human Grx2 (HsGrx2) isoforms are lengthier than HsGrx1. However, the difference is made by several alpha helixes while containing a similar number of active sites and beta sheets (Lundberg et al., 2001). HsGrx2 isoforms can be localized either in the mitochondrion (Grx2a) or nucleus (Grx2b) (Lundberg et al., 2001). HsGrx2 is highly elucidated for its functions and suggested to involve in several biological processes including iron-sulfur cluster biogenesis and redox homeostasis (Bräutigam et al., 2013). Further, HsGrx2 well-known for antiapoptotic function against H₂O₂ oxidative stress (Wu et al., 2010). Moreover, Antioxidant activity and glutathionylation activity of Grxs are highly required for activating many cells signaling pathways such as NF κ B, TLR, and AKT signaling pathways (Chantzoura et al., 2010; Daily et al., 2001; Murata et al., 2003).

In fish, Grx2 reported involving in embryogenesis, heart development, iron-sulfur cluster coordination and brain development (Berndt et al., 2014; Brautigam et al., 2013, 2011; Bräutigam et al., 2013). However, existing studies on fish Grx2 mainly focus on growth and development. There are few reports on Grx2 of aquatic organisms in immune responses (Mu et al., 2012; Zheng et al., 2019). Investigating of immune responses of different genes might be helpful for seahorse cultivation. Seahorses are tiny sea creatures that made high curiosity due to shape, life span and medicinal value (Woods, 2007). There are recognized as endangered species whereas over-exploitation for medicinal purposes can be one of threat. Therefore, the culturing of seahorses for human needs is permitted by many countries (Koldewey and Martin-Smith, 2010b). However, seahorse farming is not much successful due to their inherited weak immunity (Lepage et al., 2015). So, cultivating of seahorses in high densities is not successful in many countries. Based on the above facts, investigating of seahorse immunity can help to develop new disease control and sustainable farming strategies. Hence, this study aims to explore the involvement of Grx2 in seahorse immunity and redox homeostasis. For that, the sequence represents the highest homology to Grx2 was identified and investigated the transcriptional and functional aspects.

3.2. Materials and methods

3.2.1. Identification and bioinformatic analysis of Grx2 sequence from *Hippocampus abdominalis*

The coding sequence (CDS) that showed the highest homology to Grx2 (HaGrx2) sequence was identified from previously stipulated *Hippocampus abdominalis* transcriptome database (Oh et al., 2016). The identified HaGrx2 sequence was verified and confirmed by NCBI Basic Local Search Tools (BLAST) (Agarwala et al., 2016). The open reading frame (ORF) and amino acid sequence of protein were predicted by Unipro UGENE software (Okonechnikov et al., 2012). Signal peptides, localization prediction, and N-linked glycosylation sites were checked by Signal IP 4.0, TargetP 1.1 and NetNGlyc 1.0 online servers respectively (Emanuelsson et al., 2000; Gupta and Brunak, 2001; Petersen et al., 2011). Molecular and physiochemical properties of the sequence was identified by ExpASy ProtParam tool (Wilkins et al., 1999). The conserved domains and motifs were recognized

by the NCBI conserved domain database (NCBI CDD) (Marchler-Bauer et al., 2015). Mitochondrial processing peptidase (MPP) cleavage site was identified by MitoFates software (Fukasawa et al., 2015), and the heliQuest online server was used to examine amphipathic helix in the predicted mitochondrial target sequence of HaGrx2 (Gautier et al., 2008). The secondary structure of HaGrx2 was predicted by I-TASSER online software (Khetrapal, 2010), and the three-dimensional structure was predicted by SWISS model workbench using Protein Data Bank (PDB) template 3uiw.1 (Biasini et al., 2014). The tertiary structure of HaGrx2 protein was visualized by PyMOL 1.3 software (The PyMOL Molecular Graphics System, Version 2.0 Schrödinger, LLC). Pairwise alignment of HaGrx2 with other Grx2 orthologs was prepared by MatGAT2.0 software (Campanella et al., 2003), and Multiple sequence alignment of Grx2 orthologs were analyzed by CLC main workbench version 8.1.0 (<https://www.qiagenbioinformatics.com/>). The Phylogenetic tree was reconstructed by the neighbor-joining method (5000 bootstraps) using MEGA7 (Kumar et al., 2016).

3.2.2. Acclimatization of big-belly seahorses, tissue sampling and immune stimulation

Healthy seahorses with an average body weight of 8 g and 12 cm of body length were purchased from Marine Ornamental Fish Breeding Center (Jeju, South Korea). Fish were acclimatized in a 300 L aquarium tank with $18\pm 2^{\circ}\text{C}$ temperature and $34\pm 0.6\%$ particle salinity units (psu) for one week. Six healthy seashores (3 female, 3 male) were dissected, and 14 tissues were collected for tissue distribution analysis. Blood was collected by tail cutting, and peripheral blood cells were isolated by centrifugation at $3000\times g$ for 10 min at 4°C . All the tissue samples were snap frozen using liquid nitrogen and stored at -80°C .

Seahorses were divided into five groups for immune stimulation. LPS (Sigma, USA; $1.25\ \mu\text{g}/\mu\text{L}$), poly I:C (Sigma, USA; $1.5\ \mu\text{g}/\mu\text{L}$), *E. tarda* ($5\times 10^3\ \text{CFU}/\mu\text{L}$) and *S. iniae* ($1\times 10^5\ \text{CFU}/\mu\text{L}$) were prepared by dissolve in $100\ \mu\text{L}$ of $1\times$ phosphate buffer saline (PBS). Then individuals in each group injected with the stimulants interperitoneally, and control group injected with $100\ \mu\text{L}$ of $1\times$ PBS. After the immune stimulation, blood and liver tissues were excised from five seahorses from each group at 3, 6, 12, 24, 48, 72 h post injection (p.i.) intervals separately. Peripheral blood cells

were isolated as described in the previous paragraph. All the experiment in this study reviewed and permitted by the Animal Care and Use Committee of Jeju National University.

3.2.3. RNA isolation and cDNA synthesis

Tissues were pooled to extract the total RNA for the tissue distribution analysis (n=6), immune challenge experiment (n=5). Total RNA was extracted by RNAiso plus (TaKaRa, Japan) and purified by RNeasy spin column (Qiagen, USA). Quality and the quantity of RNA was measured by a μ Drop Plate reader (Thermo Scientific, USA) and visualized by 1.5% agarose gel electrophoresis. Isolated RNA was diluted to a final concentration of 1 μ g/ μ L, and 1st strand cDNA was synthesized by using PrimeScriptTM II cDNA Synthesis Kit (TaKaRa, Japan). Synthesized cDNA was diluted to 40-fold in nuclease-free water and stored at -80°C.

3.2.4. The mRNA expression profiling by Quantitative real-time PCR (qPCR) analysis

The mRNA expression profiles of both tissue distribution and temporal expression were determined by qPCR method using TaKaRa Thermal Cycler Dice Real Time system III (TaKaRa, Japan). All the qPCR primers were designed under the guidelines of minimum information for publication of quantitative real-time PCR experiments (MIQE) (Bustin et al., 2009). IDT PrimerQuest online Tool (<https://sg.idtdna.com>) was used to construct the qPCR primers (Table 04). The seahorse 40S ribosomal protein S7 (Accession no: KP780177) was selected as the internal reference gene. The qPCR reaction was carried out in final volume of 10 μ L containing 3 μ L of cDNA template, 1.2 μ L of nuclease-free water, 5 μ L of Ex TaqTM SYBER premix and 0.4 μ L of each primer (10 pmol/ μ L). The qPCR thermal profile started with an initial denaturation at 95°C for 10 min, followed by 45 cycles of 95°C for 5 s, 58°C for 20 s, 72°C for 20 s. After 45 cycles, a final cycle of 95°C for 15 s, 60°C for 30 s and 95°C for 15 s were set for the dissociation analysis of the target. All the reactions performed in triplicates.

The Livak ($2^{-\Delta\Delta CT}$) method was used to analyze the relative *HaGrx2* expression levels (Livak and Schmittgen, 2001). Ct value of lowest *HaGrx2* expressed tissue was used for the normalization in

tissue-specific expression analysis. For the temporal expression analysis, *HaGrx2* expression levels at different p.i. indicated as fold changes relative to the PBS control at each time point. All the data represented as mean± standard deviation (SD). In spatial expression analysis, statistical significance ($p<0.05$) of the data was evaluated by the Mann Whitney *U* test using IBM SPSS 24 statistical software (IBM, USA). Temporal expression data at each time point was statistically compared ($p<0.05$) with un-injected control by *t*-test.

3.2.5. Recombinant plasmid construction

Specific cloning primers with respective restriction sites were constructed using the IDT OligoAnalyzer tool (Table 04) (Owczarzy et al., 2008). The CDS of the *HaGrx2* was amplified using cDNA derived from brain tissue. The PCR reaction was performed by adding 2 μ L of 10 pmol/ μ L each primer, 5 μ L of 10 \times Ex Taq buffer, 4 μ L of 2.5 mM dNTP, 10 μ L of cDNA template and 0.4 μ L of 5U/ μ L Ex Taq polymerase. The PCR cycle started with an initial denaturation at 94°C for 4 min followed by 35 cycles of 94°C for 30 s, 55°C for 30 s, 72°C for 30 s and a final extension at 72°C for 10 min. Amplified PCR product was purified by Accuprep® PCR purification kit (Bioneer co., Korea). Both PCR product and the pMAL c5x vector (New England BioLabs Inc, USA) subjected to restriction digestion according to the manufacturer's protocol (TaKaRa, Japan). The digested PCR product and c5x vector purified by Accuprep® PCR purification kit and Accuprep® Gel purification kit (Bioneer Co., Korea). Then 150 ng of digested c5x fragments was ligated with 50 ng of digested PCR product by using 5 μ L of Ligation Mighty Mix (TaKaRa, Japan) at 4°C for 30 min. The ligated product was transformed into *E. coli* DH5a competent cells and colonies which were confirmed by colony PCR sent for the sequencing (Macrogen, Korea).

3.2.6. Overexpression and purification of recombinant *HaGrx2*

In order to express the r*HaGrx2* protein, recombinant vectors with confirmed sequences transformed into *E. coli* BL21 (DE3) competent cells. Cells were cultured in LB rich ampicillin medium (LB + 0.2% glucose + 100 μ g/ μ L of ampicillin) at 37°C at 200 rpm until reach to 0.5 optical

density at 600 nm. Then cultured cells were supplemented with 1 mM isopropyl β -D-1-thiogalactopyranoside (IPTG) and further incubated at 20°C for 8 h. End of the incubation, cells were harvested by centrifugation at 4°C, 3500 rpm for 30 min. The obtained cell pellet was resuspended in 25 mL of column buffer (20 mM Tris -HCl, 200 mM NaCl and 1 mM EDTA, pH 7.4). The fusion protein of rHaGrx2 and maltose binding protein (MBP) was purified by pMAL protein fusion and purification system (NEB, USA) based on manufacturers protocol. The concentration of eluted protein was measured by Bradford's method. Protein banding pattern and the purity of the purified protein was observed by 12% SDS-PAGE. The recombinant protein was stored at -80°C for future use.

3.2.7. Functional assays

3.2.7.1. HaGrx2 deglutathionylation activity corresponds to the Human Grx1

HaGrx2 deglutathionylation was measured by fluorescent glutaredoxin assay kit 96 well (IMCO cooperation Ltd, Sweden) according to the manufacturer's protocol. Samples were prepared by using 1 nM of rHaGrx2. Additionally, a control sample was prepared by replacing rHaGrx2 with 1 nM MBP. Fluorescence measured by SYNERGY/HT™ microplate reader (Biotek, Korea)

3.2.7.2. Oxidoreductase activity of HaGrx2

a). insulin disulfide reduction activity

Insulin disulfide reduction activity of rHaGrx2 was measured at 650 nm as described previously (Zaffagnini et al., 2008). The reaction was performed in a 96 well plate, and the reaction mixture consisted of the final volume of 200 μ L containing 100 mM potassium phosphate buffer (pH 7.9), 2 mM bovine insulin, 2 mM EDTA and various concentrations of rHaGrx2 (0, 25, 50 μ g/mL). Insulin aggregation initiated by adding 0.1 M dithiothreitol, (DTT) (Sigma, USA). The insulin aggregation rate at 650 nm was recorded with 5 min intervals by Multiskan Sky microplate reader (Thermo Scientific, USA). The treatments were statistically compared with control (0 μ g/ μ L HaGrx2 + DTT) by independent *t*-test using IBM SPSS statistics 24 software.

b.) L-dehydroascorbic (DHA) reduction assay.

DHA reduction activity of rHaGrx2 was analyzed as described in Wells *et al.* by measuring the decrease in the absorbance at 340 nm (Wells et al., 1990). Reaction was performed in 200 μ L reaction mixture containing 2 mM EDTA, 0.2 mM NADPH, 0.1 μ g/mL glutathione reductase, 1 mM GSH and different concentrations (0, 1, 2 mM) of DHA (Sigma, USA). The enzymatic reaction was initiated by adding 20 μ g/mL rHaGrx2. Then the absorbance measured for 2 min with 30 sec intervals.

3.2.7.3. Cell culture and transfection of HaGrx2

HaGrx2 was cloned into mammalian expression vector pcDNA3.1 (+) using *KpnI* and *EcoRV* restriction sites (Table 04). Plasmid construct was verified by sequencing and purified by QIAfilter™ Plasmid Midi Kit (Qiagen, Germany). Fathead minnow (FHM) epithelium cells were cultured in Leibovitz's L-15 medium added with 10% fetal bovine serum (FBS) and 1% streptomycin and penicillin. Cells were seeded at a concentration of 3×10^5 cell/mL in 96-well plate and incubated at 25°C for 24 h. Then the recombinant plasmid and empty pcDNA3.1 (+) vector (1 μ g) were transfected into Fathead minnow (FHM) epithelium cells using X-tremeGENE™ 9 reagent based on the manufacturer's protocol.

Table 4: Primers used in cloning and qRT-PCR of HaGrx2

Primer Name	Sequence 5' - 3'	Description
ShGrx2 qPCR forward	CGATGACGGCAGGAGATTAC	T _m 62°C, 135 bp
ShGrx2 qPCR reverse	ACTAACTTGCCCTGCTGATG	T _m 62°C, 135 bp
40S ribosomal S7 qPCR forward	ACTCTGGAAGTGGCAGAGGAAGAC	T _m 60 °C, 187 bp
40S ribosomal S7 qPCR reverse	TGAAGTCATTCATGTTGGTGGCCTGTA	T _m 60 °C, 187 bp
ShGrx2 cloning forward	GAGAGAgatataTGTTTTCTCGAGCCGGATGCTG	T _m 59.8°C, 433 bp, c5x, <i>EcoRV</i>
ShGrx2 cloning reverse	GAGAGAgattcTCATTTTGCAGATTTCGAATCGTCCGC	T _m 59.9°C, 433 bp, c5x, <i>EcoRI</i>
ShGrx2 cloning forward	GAGAGAggtaccATGTTTTCTCGAGCCGGATGCTG	T _m 59.8°C, 433 bp, pcDNA, <i>KpnI</i>

3.2.7.4. Cell viability assay upon H₂O₂

Cells were incubated different H₂O₂ concentrations (0, 200, 500μM) for 24 hrs. Then 50 μL of 4 mg/mL 3-(4,5-dimethylthiazol-2-yl)-2, 5-diphenyltetrazolium bromide (MTT) was added to each well and incubated for 2 h. The supernatant was removed by aspiration, and 150 μL of dimethyl sulfoxide (DMSO) was added to each well to dissolve the formazan crystals. Then the absorbance of the reaction mixture was measured at 570 nm using the Multiskan Sky microplate reader (Thermo Scientific, USA). Microscopic observation of cell in each treatment was done by Leica DFC425C digital microscope.

3.3. Results

3.3.1. Bioinformatic analysis of HaGrx2

The coding sequence of identified Grx2 sequence (accession No. MK936322) was 466 bp and encoded 152 amino acids. The predicted amino acid sequence does not contain a signal peptide or N-linked glycosylation sites. The predicted molecular weight of the HaGrx2 amino acid sequence was 16.4 kDa, and theoretical pI was 8.88. As depicted in Figure 9, HaGrx2 protein consisted of glutaredoxin domain (48-129 aa) and thioredoxin/glutaredoxin CXXC active motif as ⁵⁶CPYC⁵⁹. Further, it contained 11 GSH binding sites. HaGrx2 contained mitochondrial targeting peptide and MPP cleavage site (Figure 9). Moreover, MTS consisted of an amphipathic helix (Figure 10A). According to the predicted tertiary structure, HaGrx2 has the classical glutaredoxin structure with four β sheets that surrounded by five α helices. The PDB template 3uiw.1. A (zebrafish Grx2) covers 76% of the 3D structure of HaGrx2 (Figure 10B). However, this 3D model does not cover all the sequences (1-27aa and 132-151 aa). According to the predicted secondary structure (Figure 9), HaGrx2 contain more than six α helices and characteristic four β sheets.

Grx2 from *Hippocampus comes*, showed the highest identity (95.4%) and similarity (96.7%) with HaGrx2 (Table 05). Grx2 of *Danio rerio* has 63.4% of identity and 75.7% of similarity with HaGrx2. According to the multiple sequence alignment, most of the amino acids are conserved in Grx2 orthologs. Grx2 from *Hippocampus comes*, and *Lates calcarifer* showed more conserveness with HaGrx2 compared to rest of selected species. CXXC motif was conserved to all the selected

species and represented as CPYC in selected fish species. As showed in Figure 11, out of 11 sites, two GSH binding sites were unique to selected fish species and the rest of the sites conserved in all the selected Grx2 orthologs. According to the phylogenetic tree (Figure 12), selected Grx1 and Grx2 orthologs make distinct 2 clusters. HaGrx2 clade with Grx2 orthologs from fish and closely clustered with Grx2 from *Hippocampus comes*.

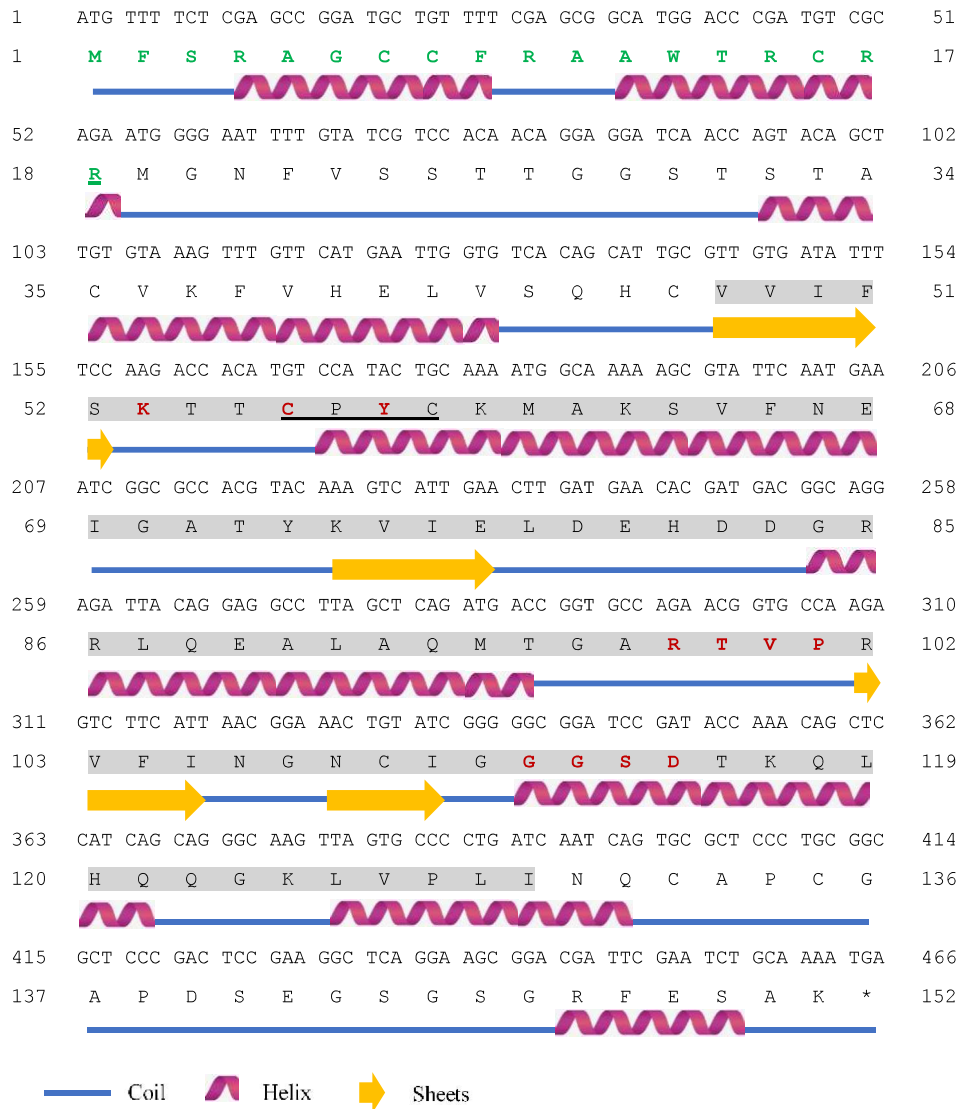
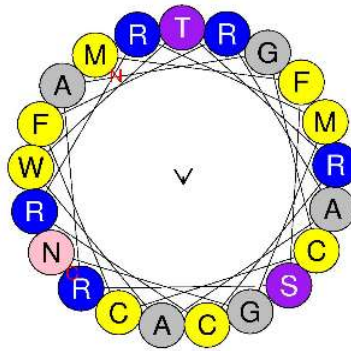


Figure 9: Sequence figure of HaGrx2

(A). Nucleotide sequence deduced amino acid sequence and predicted secondary structure of HaGrx2. Green color letters indicate the predicted mitochondrial processing peptide (MPP). The green color underlined letter denotes the cleavage site for MPP. Predicted glutaredoxin domain headed with gray color and CXXC motif underlined with black color. GSH binding sites are marked with bold red color letters.

A



B

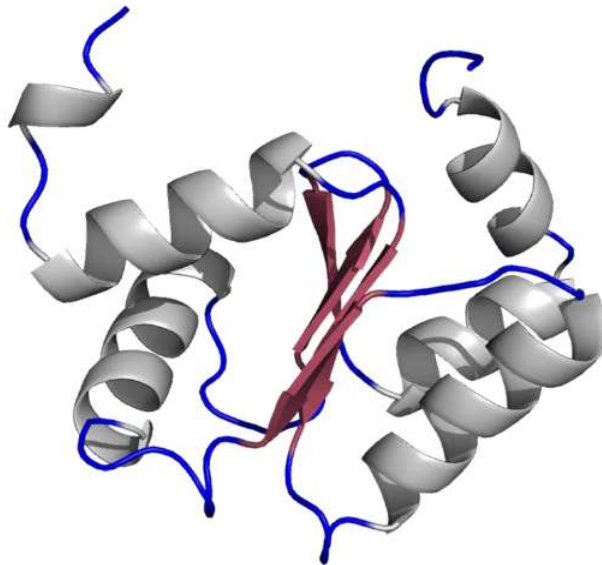


Figure 10: predicted amphipathic helix and predicted tertiary structure of HaGrx2
(B). Predicted amphipathic helix in MPP of HaGrx2. (C) Predicted tertiary structure for HaGrx2 using 3uiw.1. A PDB template

Table 5: Identity and similarity percentages of HaGrx2 with other Grx2 orthologs from different species

Accession No	Scientific name	Identity (%)	Similarity (%)
XP_019727358.1	<i>Hippocampus comes</i>	95.4	96.7
XP_018526333.1	<i>Lates calcarifer</i>	76.2	81.4
XP_019958097.1	<i>Paralichthys olivaceus</i>	69.7	77.0
NP_001002404.1	<i>Danio rerio</i>	63.2	73.5
XP_023284517.1	<i>Seriola lalandi dorsalis</i>	62	66.1
PKK27918.1	<i>Columba livia</i>	42.1	60.5
XP_020646120.1	<i>Pogona vitticeps</i>	41.1	55.7
XP_025141889.1	<i>Bubalus bubalis</i>	41.1	55.2
NP_001230646.1	<i>Sus scrofa</i>	38.7	53.6
AAI09743.1	<i>Bos taurus</i>	38.4	55.2
NP_001016637.1	<i>Xenopus tropicalis</i>	38.2	55.3

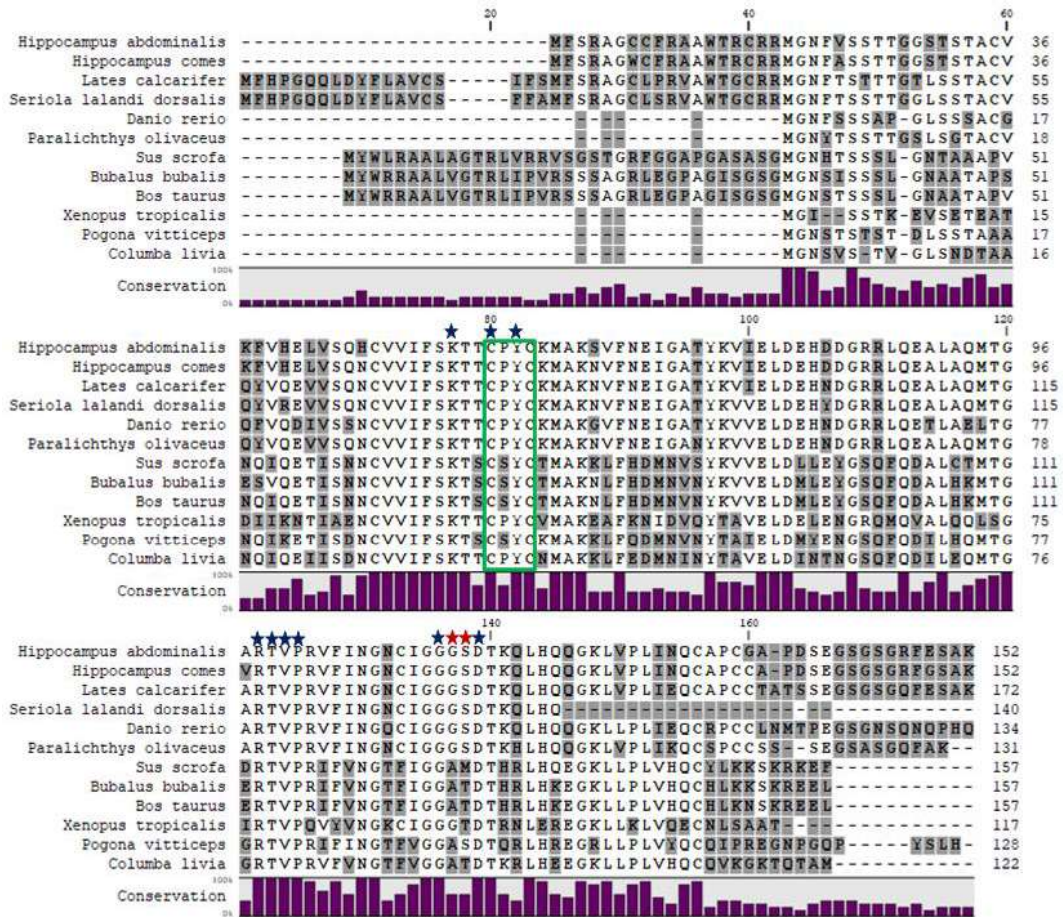


Figure 11: multiple sequence alignment of Grx2 orthologs

Non-conserved residues are shaded in gray. Conservation percentage represented as a bar plot. The conserved CXXC motif is marked with a green box, and GSH binding sites that are conserved in HaGrx2 and all other selected organism are marked with asterisks. GSH binding sites that are conserved only in selected fish species are marked with a red color asterisk. Accession numbers of selected protein sequences are listed in Table 2.

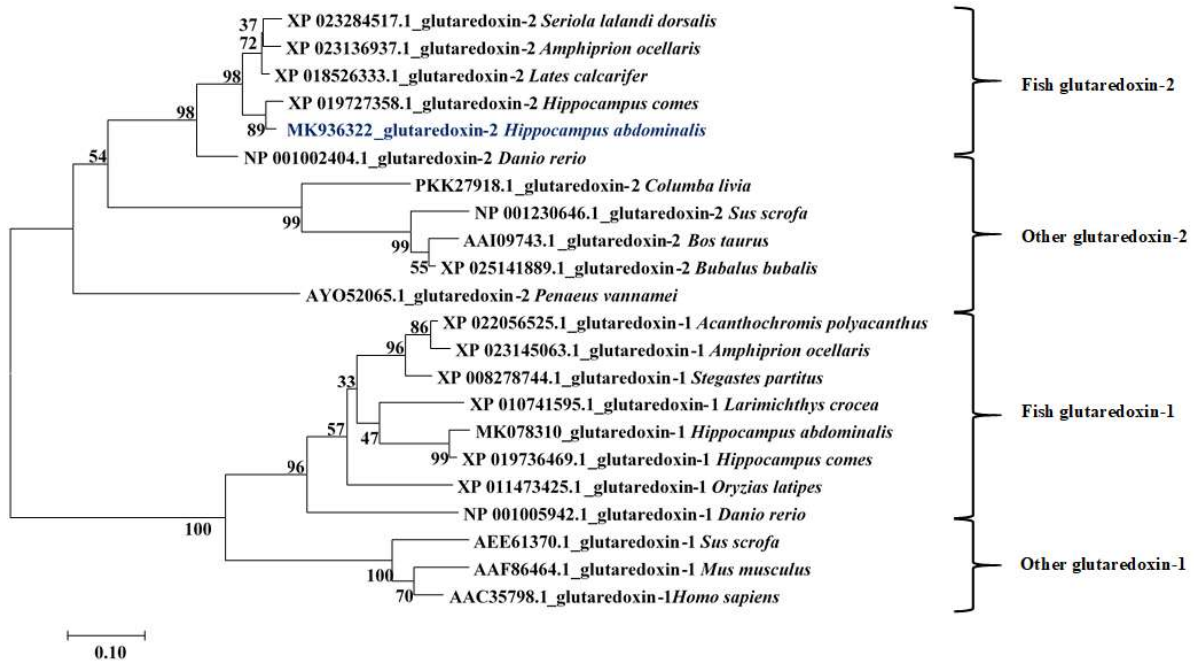


Figure 12: Phylogenetic reconstruction of *HaGrx2*
 Bootstrap support values corresponding to each branch are indicated.

3.3.2. Spatial and temporal expression profile of *HaGrx2*

As shown in Figure 13, *HaGrx2* was ubiquitously expressed in 14 tissues selected. The highest expression of *HaGrx2* was observed in skin and brain whereas lowest expression found in the liver. Temporal expression of blood *HaGrx2* upon LPS stimulation showed dynamic modulation throughout the p.i intervals (Figure 14A). However, the highest *HaGrx2* upregulation can be observed at 72h p.i upon LPS, Poly I:C and *E. tarda* stimulants. For the *S. iniae* infection, *HaGrx2* showed dynamic regulation, and highest expression can be seen in 48 h p.i.

When considering the *HaGrx2* expression in liver, dynamic modulation upon LPS, *S. iniae* stimulation (Figure 14B) was observed. For Poly I:C and *E. tarda*, highest *HaGrx2* expression was observed at 48 h p.i. Significant *HaGrx2* upregulations were detected at 24 h, 48 h, and 72 h p.i upon *S. iniae*.

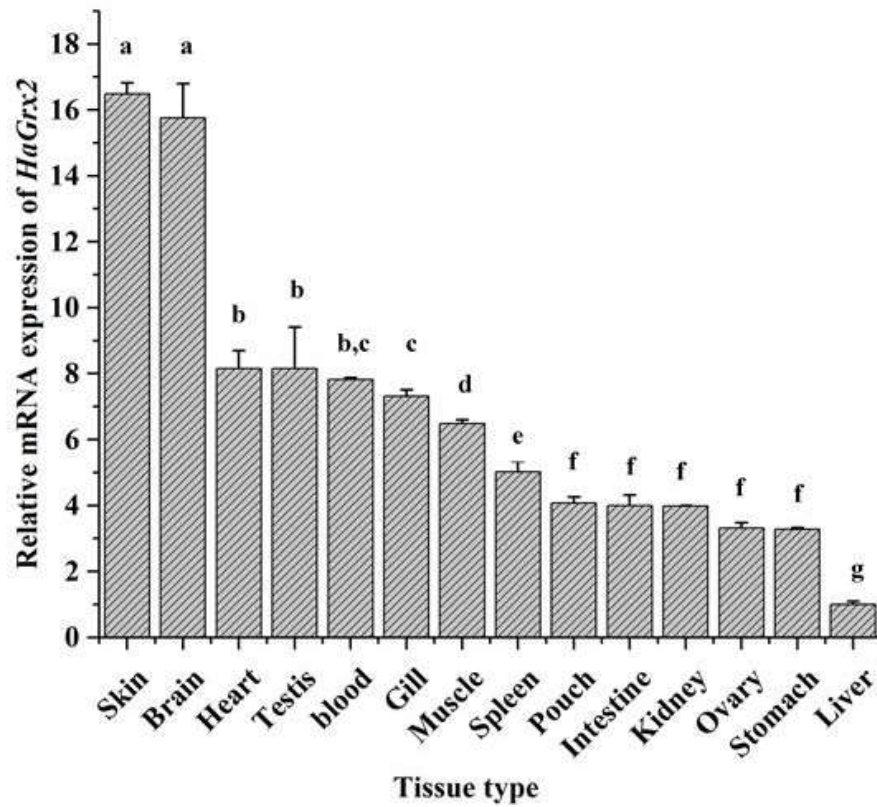
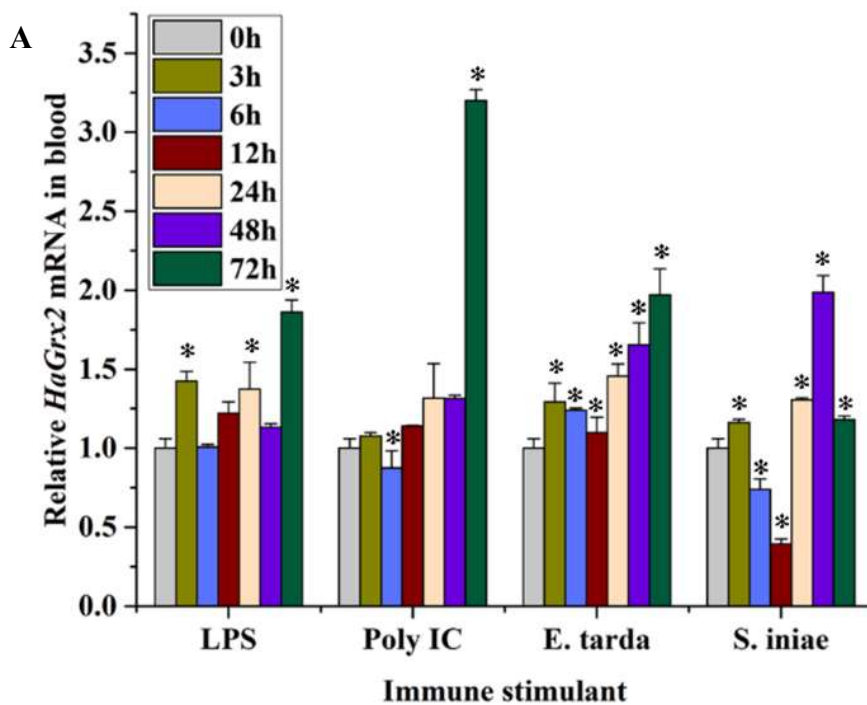


Figure 13 Tissue-specific expression profiles of HaGrx2

The data are represented as mean values ($n = 3$) \pm S.D. Significant differences in expression among tissues are indicated with different letters ($p < 0.05$).



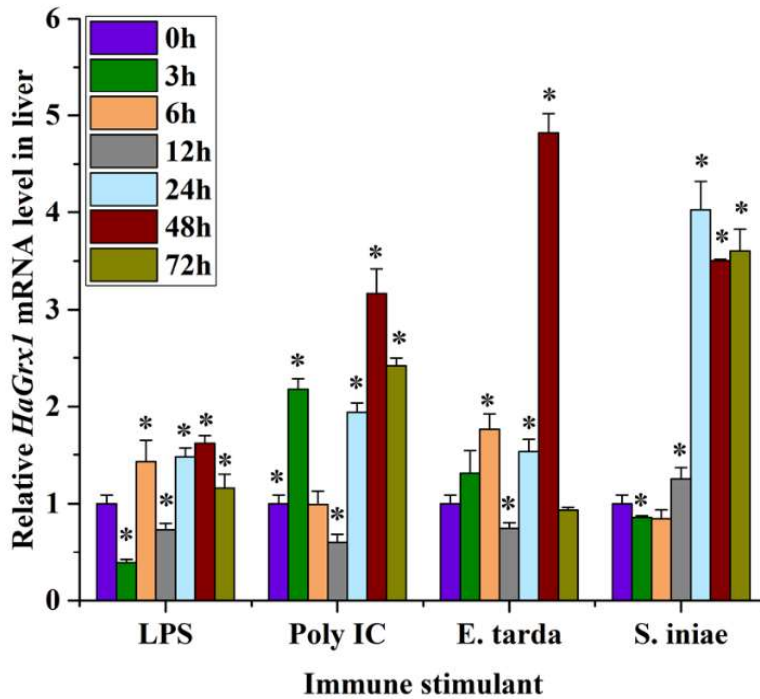


Figure 14: Temporal expression profiles of HaGrx2 in blood and liver

Temporal expression profiles of HaGrx2 in (B) blood (C) Liver after LPS and poly I:C, *Edwardsiella tarda* and *Streptococcus iniae* challenges. The data are represented as mean values ($n = 3$) \pm S.D. Significant differences compared to the blank (0 h) are indicated with an asterisk for $p < 0.05$.

3.3.3. Overexpression and purification of rHaGrx2 as MBP fusion protein

According to the SDS PAGE gel image (Figure 15), expressed rHaGrx2-MBP fusion protein can be recognized as a single band between 50 kDa and 70 kDa. The expected rHaGrx2-MBP fusion size was ~58 kDa (16.4 kDa + 42 kDa).

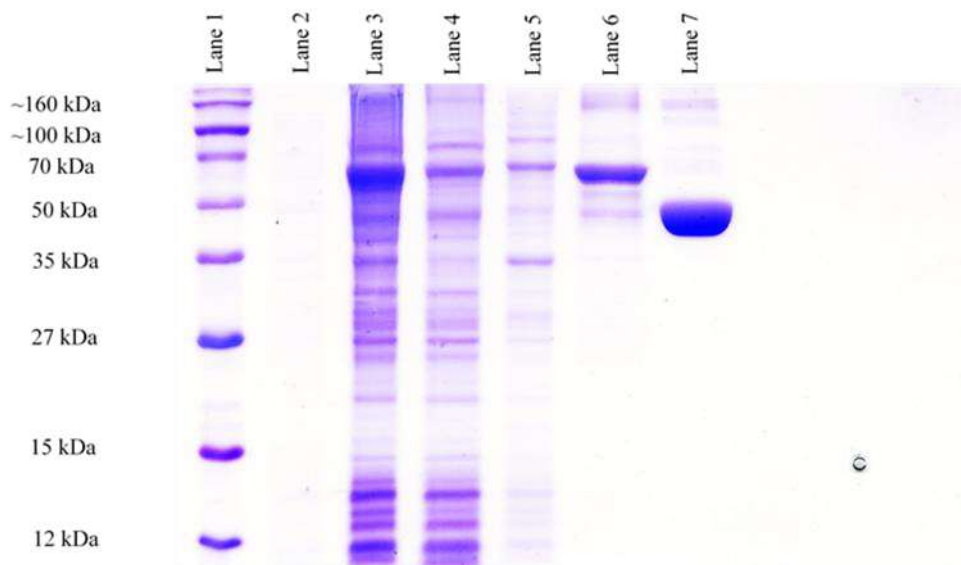


Figure 15: SDS-PAGE analysis of overexpressed HaGrx2 in *E. coli*

The SDS-PAGE analysis of overexpressed and purified HaGrx2 as an MBP-fusion protein. Lane 1: unstained protein ladder, Lane 2: crude extract of uninduced *E. coli* BL21 cells, Lane 3: crude extract of induced *E. coli* BL21 cells, Lane 4: supernatant after sonication and centrifugation of induced *E. coli* BL21 cells, Lane 5: Pellet, Lane 6: purified HaGrx2 fusion protein, Lane 7: Purified MBP protein.

3.3.4 Functional studies

3.3.4.1. The deglutathionylation activity of rHaGrx2 correspond to the human Grx1

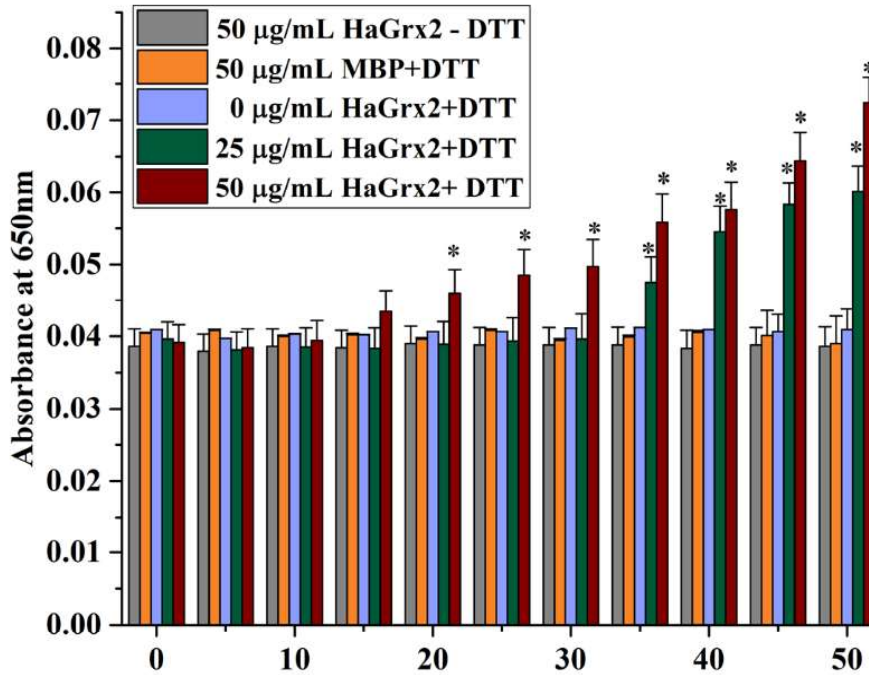
According to the data obtained from fluorescent glutaredoxin kit, 1 nM of rHaGrx2 correspond to 0.84 nM of active HsGrx1.

3.3.4.2. Oxidoreductase activity of rHaGrx2

Oxidoreductase activity of HaGrx2 was assessed by Insulin aggregation assay. As depicted in Figure 16A, significant insulin disulfide reduction activity was observed after 20 min in rHaGrx2+DTT treated samples. Higher insulin reduction activity was detected in 50 µg/mL rHaGrx2+DTT sample than the 25 µg/mL rHaGrx2+DTT sample. Except for rHaGrx2+DTT treated samples, other samples did not contain significant insulin reduction activity.

DHA reduction activity of rHaGrx2 was measured as NADPH turnover at 340 nm. According to Figure 16B, rHaGrx2 contain significant DHA reduction activity and it was increased with DHA concentration. MBP control and 0 mM DHA samples did not show activity at 340 nm.

A



B

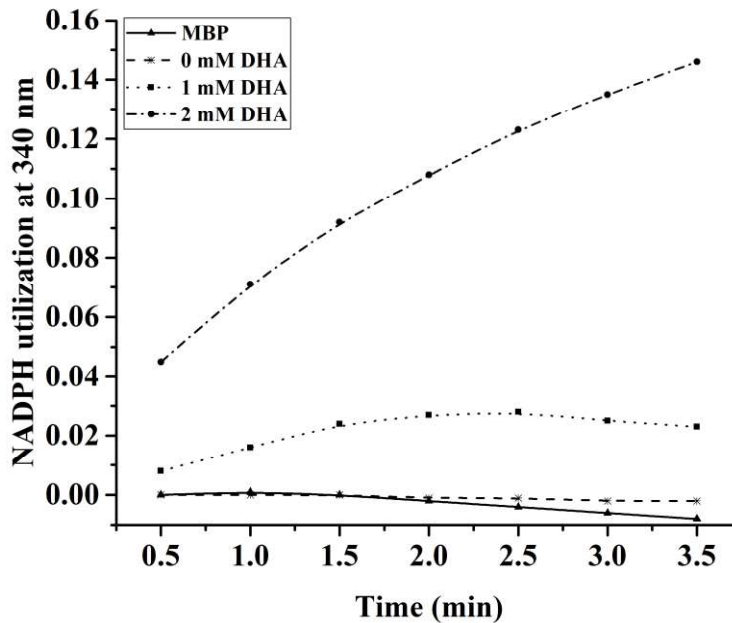


Figure 16: Insulin aggregation and dehydroascorbic acid reduction activity of rHaGrx2

(A) DHA reduction activity of rHaGrx2 with different DHA concentration at 25°C. (B) Insulin disulfide reduction activity of rHaGrx1 with different protein and DTT combinations. Data were obtained from triplicates and are expressed as mean values \pm S.D. Significant differences ($p < 0.05$) compared to control ($0\mu\text{g/mL}$ rHaGrx1+DTT) are indicated by *.

3.3.4.3. Cytoprotective activity upon oxidative stress

The cytoprotective activity of HaGrx2 was examined through cell viability upon H_2O_2 treatment. As shown in Figure 16, HaGrx2 transfected cells showed significant cytoprotective activity compared to pcDNA transfected cells and control cells.

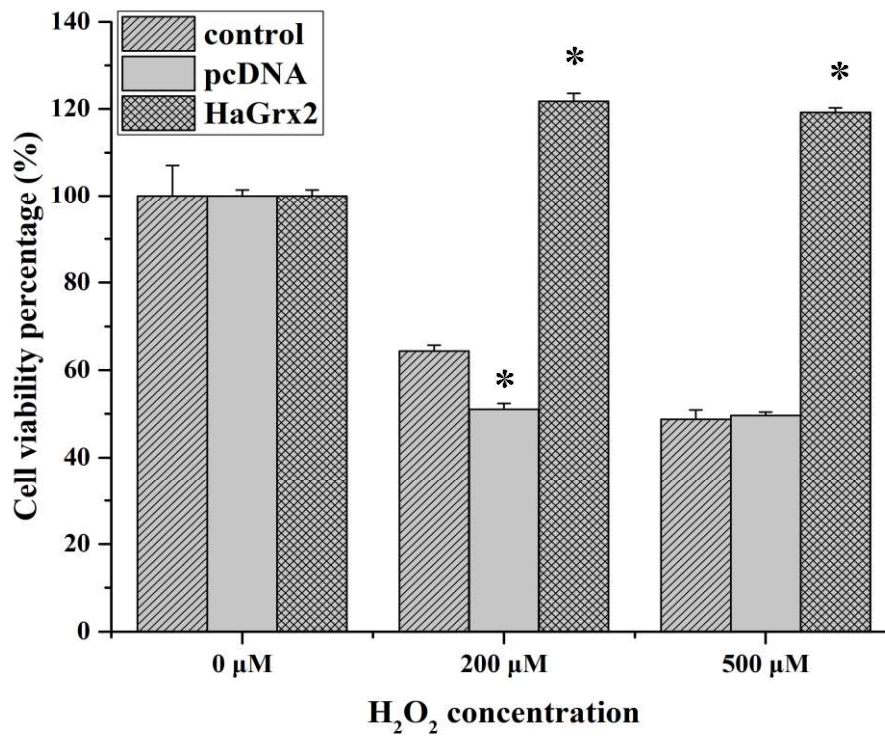


Figure 17: percentage cell viability upon H_2O_2 stress.

Percentage viability of non-transfected, pcDNA and HaGrx2 transfected FHM cells upon H_2O_2 stress. Significant differences of treated samples compared to the control at each treatment are indicated with an asterisk ($P < 0.05$).

3.4. Discussion

Grxs are well-known for its abundance in organisms and can be found in varieties of isoforms. These isoforms share a typical thioredoxin-like structure and mainly involved in cellular redox homeostasis. However, functional aspects of Grxs orthologs show significant variations and expressed in different organelles in cells. For example, mammalian Grx1 can be found in the cytosol and has profound oxidoreductase activity. Recently discovered Mammalian Grx2 has been reported

for its expression in mitochondrial and nucleus while consist of sound peroxidase activity (Fernando et al., 2006). When considering fish Grx2, there are four comprehensive studies based on the development of zebrafish. However, the importance of redox activity of fish Grx2 upon immunity need to be discussed further. Therefore, in this study, we perform several functional assays related to redox activity and immunity.

3D structure of Grx2 from *Danio rerio* (3uiw.1. A) showed 81.03% sequence identity with the 3D structure of HaGrx2. However, this PDB model does not predict the full N-terminal (26 aa) and C-terminal (17aa) structure of the HaGrx2. Therefore, we predict the secondary structure of HaGrx2, and the new structure has additional α helixes while remaining the same number of β sheets as in 3uiw.1. A PDB model. However, limited data from fish species other than zebrafish, make some difficulties in making a comparison with HaGrx2 3D structure.

The deduce HaGrx2 shows typical characteristics with Grx2 from other species. Though the length of Grx2 orthologs shows considerable variations, glutaredoxin domain shows more conserved features in selected Grx2 sequences. The C-terminal and N-terminal counterparts of the Grx2 orthologs show less conserved features. HaGrx2 exhibit more than 75% of similarity and 60% of identity with fish Grx2 sequences. Further, 11 GSH binding sites found in HaGrx2 are conserved to selected fish Grx2 orthologs. Even in the phylogenetic tree, HaGrx2 tightly cluster with fish Grx2 sequences. Therefore, we can conclude that HaGrx2 shares conserve features with fish and can predict unique activities. For example, previously published reports suggest that Grx2 involve in critical developmental processes in fish. Zebrafish Grx2 (ZfGrx2) regulate heart, vascular, neural and brain development of zebrafish embryo (Berndt et al., 2014; Brautigam et al., 2013, 2011). ZfGrx2 knockdown studies show it can severely affect the development of the embryo.

In vertebrates, there are four major Grx paralogs can be found. Grx 1 and Grx2 known as dithiol glutaredoxins and Grx3 and Grx5 known as monothiol glutaredoxins (Hanschmann et al., 2013b). According to the phylogenetic tree, HaGrx1 and HaGrx2 paralogs distinctly clade with fish Grx1 and fish Grx2 respectively. Further, they tightly clustered with *Hippocampus comes* Grxs. It is reported that homology between HsGrx1 and HsGrx2 is 36%. However, pairwise comparison of

HaGrx1 (Gladyshev et al., 2001) and HaGrx2 share much lower identity (24.5%) and similarity (34.6%). Therefore, Functional aspects of HaGrx2 can be more related to Grx2 orthologs.

HaGrx2 does not possess any signal peptide or n-linked glycosylation sites, but it has a mitochondrial targeting sequence (MTS). Many of mitochondrial proteins are produced in the nucleus and translocate into mitochondria. As these proteins produce in one subcellular organelle and translocate to another, they possess target signals that help for the translocation and folding mechanisms (Fox, 2012). Typically, MTS is a cleavable peptide in N-terminal with approximately 15-70 residues that form amphipathic helix (Gakh et al., 2002). HsGrx2a is a mitochondrial Grx isoform which has MTS. Lundberg *et al.* reported that MTS of HsGrx2a is rich with positively charged and hydrophobic amino acids and contain MPP site. Further, the predicted secondary structure of HsGrx2a was folded into an amphipathic helix (Lundberg et al., 2001). The predicted MTS for HaGrx2 contains MPP cleavage site as well as represent characteristics of the amphipathic helix. Hence, bioinformatic evidences suggest that HaGrx2 is a mitochondrial protein similar to other Grx2 in the vertebrates.

According to the tissue distribution analysis, highest expression found in skin and brain. The function of Grx2 in fish skin is not clear but studies that prove vertebrate Grx2 mainly involve in redox homeostasis of epithelial cell lines (Fernando et al., 2006; Wu et al., 2011, 2010). Knockdown of mouse Grx2 showed increased sensitivity for oxidative stress in lens epithelial cells (Wu et al., 2011). Skin is the largest organ of the body and separate internal and external environment of live fish. It acts as the first line defense against many microorganisms and chemicals. Therefore, ROS produced during the cell functions need to be neutralized by antioxidant proteins. Further, the skin is essential for the osmotic balance of fish and skin epithelial cells involved in wound healing mechanisms of fish cells (Ángeles Esteban and Cerezuela, 2015). Therefore, the epithelial cells present in the skin are more metabolically active. The requirement of high energy for physiological and immune functions increase the ROS production in mitochondria. Hence, the peroxidase activity of Grx2 might be required continuously in fish skin.

It is suggested that the brain represent 0.1%-1% of the total weight of vertebrates but consume 2.7%-3.4% of the energy of ectothermic vertebrates' metabolism. The brain is highly active in fish as brain cells are contacted with motor neurons and directly influence the tail movement of fish ("Division of labour in the fish brain | Max-Planck-Gesellschaft," n.d.). Seahorse has a prehensile tail that involves both motion and attachment to substrates. Therefore, a higher energy requirement can be expected in brain tissue for the motion. Mitochondrial complex I in brain catalyzes the first step of the mitochondrial electron transport chain (Lenaz et al., 2006). Complex I contain active thiol groups that are sensitive to the redox status of the cell. The factors required for the maintenance of complex I under normal and oxidative stress conditions are not well defined. However, it is reported that downregulation of Grx2 in the brain can potentially inhibit the Complex I activity in human and mouse models (Karunakaran et al., 2007). Therefore, Grx2 regulate the functional integrity of the mitochondrial complex I under normal physiological conditions and highest expression of *HaGrx2* transcripts in brain tissues can be explained by the above facts.

Presence of ROS and reactive nitrogen species make proteins susceptible to irreversible oxidation by producing sulfinic and sulfonic acids (Lo Conte and Carroll, 2013). Therefore, thiol-containing proteins undergone to intermolecular bonds with GSH or other thiol-containing proteins (glutathionylation) (Grek et al., 2013). Glutathionylated proteins have different structural and functional aspects than native protein (Belcastro et al., 2017). It acts as a protective mechanism for proteins, but the functionality of the proteins can be restored by deglutathionylation by glutaredoxin. This mechanism can be observed in mitochondrial complex I as it is a thiol-containing protein. Glutathionylation of complex I prevent its irreversible impairment due to H_2O_2 and reduce the ROS production (Wu et al., 2010). Mitochondrial ROS activate both antiviral and antibacterial activity as innate immune responses (Chen et al., 2018; Pourcelot and Arnoult, 2014; Ray et al., 2012). On the other hand, excessive level of ROS can lead to impairment of several proteins and subsequently lead to cell apoptosis, necrosis and cell death (Di Meo et al., 2018). Therefore, mitochondrial ROS emission should be regulated precisely. During the high oxidative stress, complex I stay in glutathionylated form and activity can be restored by Grx2 thus ROS production rate maintained

(Wu et al., 2010). Therefore, Grx2 act as a signaling switch in H₂O₂ mediated cell signaling and innate immune responses. According to the literature, major ROS producing sources in mitochondria is regulated by Grx2 (Chalker et al., 2018).

During a bacterial infection, macrophages engulf the bacteria by phagocytosis. Then bacteria are lysed and release the PAMP that can bind with TLRs (Kaufmann and Dorhoi, 2016). It is reported that LPS and lipoteichoic acid (PAMP in gram-positive bacteria) can elevate the mitochondrial ROS production in macrophages (West et al., 2011). Not only the white blood cells, but erythrocytes of fish also reported for phagocytosis activity (Passantino et al., 2002). Therefore, ROS production in peripheral blood cells against PAMP and bacterial challenge capable of activating the cell signaling pathways. Hence Grx2 activity in peripheral blood cells may be the regulating the ROS producing sites and restore the proteins undergone to S-glutathionylation. However, the mechanism of precisely maintain the ROS level by Grx2 is not clear because redox regulation by Grx2 is complex and depend on the type of tissues and various factors. Based on the above facts, the dynamic regulation of HaGrx2 transcripts upon PAMP and bacterial stimulation in the blood can be expected. Apart from bacterial PAMP, Poly I:C (viral mimic) identify by the TLR3. TLR3 induces ROS generation lead to inflammatory responses that essential for STAT1 activation (Yang et al., 2013). Therefore, ROS homeostasis activity of Grx2 required in macrophages for anti-viral innate immune responses.

The same scenario was observed in the liver because of Grx2 act as a critical regulator of ROS producing complexes. It is reported that complex I, pyruvate dehydrogenase and 2-oxoglutarate dehydrogenase also act as ROS releasing site in liver mitochondria which deglutathionylating by Grx2 (May et al., 1997). As Grx2 induce the activity of Complex I, pyruvate dehydrogenase and 2-oxoglutarate dehydrogenase higher expression of Grx2 in the liver can be expected (Chalker et al., 2018). However, Liver *HaGrx2* showed significant fold expression for live gram-positive bacteria than PAMP stimuli. It is reported that Kupffer cells can directly bind to lipoteichoic acid in gram-positive bacteria (Llorente and Schnabl, 2016). Therefore, the liver involves in fast elimination of pathogens from the blood. As hepatocytes straightly involve in the clearance of live pathogens, ROS

mediated antibacterial and antiviral activity might highly require in the liver. Hence significant Grx2 expression can be observed in both blood and liver upon immune stimulation.

As described previously, the deglutathionylation activity of Grxs are critical for cellular functions. There are many identified proteins undergone to deglutathionylation by Grxs. Serum albumins are abundant plasma protein that contains ROS scavenging activity, ion binding, transport activity, and antiapoptotic activities. It contains free cysteine residues that responsible for the functionality of the protein. During higher oxidative stress, free cysteine in serum albumin susceptible for the S-glutathionylation. Hence, deglutathionylation of fluorescent BSA-SSG was measured using HsGrx1 standard curve. Therefore, HaGrx2 is comparable with HsGrx1 and showed little lesser activity than HsGrx1. However, Lundberg *et al.* suggested that HsGrx2 exhibit only 10% specific activity compared to HsGrx1 (Lundberg *et al.*, 2001). Therefore, we can predict that HaGrx2 represent higher activity than HsGrx2. The primary reason for the higher activity in HaGrx2 might be amino acid residues present in the catalytic motif. Most mammalian Grx1 contain CPYC as a catalytic motif, and Grx2 consisted of CSYC. Foloppe *et al.* Replacement of proline residue in the Grx catalytic motif by serine can severely affect the redox properties (Foloppe and Nilsson, 2004). HaGrx2 contain CPYC as the catalytic motif which similar to HsGrx1. Hence, HaGrx2 contain significant deglutathionylation activity.

Matured insulin consisted of two chains named A and B (Weiss *et al.*, 2000). Both chains linked by inter-chain disulfide bonds and can be precipitated by reduction. Insulin precipitation assay is commonly used to measure the disulfide reduction activity of thioredoxin (Holmgren, 1979). In this assay, DTT used as the electron donor for the HaGrx2. It is reported that HsGrx2 can accept electrons from sources such as thioredoxin reductase other than GSH (Johansson *et al.*, 2004). Though it has been accepted that Grxs have minor insulin reduction activity, HaGrx2 exhibit significant insulin reduction activity with DTT.

Ascorbic acid is a powerful antioxidant present in many organisms but teleost fish lack of ability to produce ascorbate due to L-gulonolactone oxidase (Ching *et al.*, 2015). Therefore, it is essential to include vitamin C to teleost fish feed unless developing Vitamin C deficiencies such as

impaired wound healing, reduced growth, scoliosis, low immunity, retard embryonic and larval development. Further, it is reported that, myoblast proliferation, migration, and differentiation (Duran et al., 2019). Moreover, ascorbate act maintains the redox homeostasis (Wilson and Wilson, 2002). Therefore, other than taking vitamin C from the feed, fish should have a proper recovering method of oxidized ascorbic to ascorbate. Glutathione S-transferase omega (GSTO) is one of the well-known protein that converts DHA to ascorbic acid. Many studies suggested that Grxs also contain dehydroascorbic reduction activity (Wells et al., 1990). HaGrx2 also contain sound DHAR activity. Hence, we can propose that HaGrx2 regulate both redox and physiological activities in seahorse.

The antiapoptotic activity of Grx2 against H_2O_2 is widely studied in mammalian models(Wu et al., 2011, 2010). According to the reports, cytoprotective activity achieved by Grx2 in various ways. Healthy epithelial cell viability decreases with H_2O_2 stress due to BAX upregulation, BCL-2 downregulation, Caspase 3 activation, and Cytochrome C escape (Wu et al., 2010). Overexpression of Grx2 was able to sustain the BCL-2 level even with the oxidative stress. Cytochrome C leakage to the cytosol from mitochondria also known as a hallmark of apoptosis. Grx2 overexpression avoids the Cytochrome C release from mitochondria (Enoksson et al., 2005). Procaspase 3 convert to Caspase 3 due to stress-induced apoptotic signals. Grx2 overexpression in epithelial cells prevents the procaspase cleavage. Further, it was identified that complex I activity severely inhibited by the H_2O_2 (Lenaz et al., 2006). Grx2 capable of preserving the complex I activity directly by deglutathionylation (Kenchappa and Ravindranath, 2003). Further, the peroxidase activity of Grx2 also can reduce H_2O_2 stress by utilizing glutathione or thioredoxin reductase (Fernando et al., 2006). On the other hand, knockdown studies of Grx2 showed greater susceptibility to oxidative stress (Wu et al., 2011). HaGrx2 also exhibit sound cytoprotective activity upon H_2O_2 treatment. Therefore, we can predict that Grx2 act as an excellent antioxidant that alleviates oxidative stress-induced cell apoptosis.

According to the functional transcriptional and molecular investigations carried out in this study, HaGrx2 possess typical glutaredoxin structure. There are bioinformatical evidences that it

could be a mitochondrial protein. Moreover, HaGrx2 has sound oxidoreductase and deglutathionylation activity. Spatial and temporal expression profiles revealed that it has potential involvement in physiological and immunological responses of seahorse. Most importantly, HaGrx2 exhibit cytoprotective activity against H₂O₂ induced oxidative stress. As a conclusion, results in this study may provide sufficient evidence of HaGrx2 and its possible functions in redox homeostasis as well as host immune responses.

References

- Agarwala, R., Barrett, T., Beck, J., Benson, D.A., Bollin, C., Bolton, E., Bourexis, D., Brister, J.R., Bryant, S.H., Canese, K., Charowhas, C., Clark, K., Dicuccio, M., Dondoshansky, I., Federhen, S., Feolo, M., Funk, K., Geer, L.Y., Gorelenkov, V., Hoepfner, M., Holmes, B., Johnson, M., Khotomlianski, V., Kimchi, A., Kimelman, M., Kitts, P., Klimke, W., Krasnov, S., Kuznetsov, A., Landrum, M.J., Landsman, D., Lee, J.M., Lipman, D.J., Lu, Z., Madden, T.L., Madej, T., Marchler-Bauer, A., Karsch-Mizrachi, I., Murphy, T., Orris, R., Ostell, J., O'sullivan, C., Panchenko, A., Phan, L., Preuss, D., Pruitt, K.D., Rodarmer, K., Rubinstein, W., Sayers, E., Schneider, V., Schuler, G.D., Sherry, S.T., Sirotkin, K., Siyan, K., Slotta, D., Soboleva, A., Soussov, V., Starchenko, G., Tatusova, T.A., Todorov, K., Trawick, B.W., Vakarov, D., Wang, Y., Ward, M., Wilbur, W.J., Yaschenko, E., Zbicz, K., 2016. Database resources of the National Center for Biotechnology Information. *Nucleic Acids Res.* 44, D7–D19. <https://doi.org/10.1093/nar/gkv1290>
- Agarwala, R., Barrett, T., Beck, J., Benson, D.A., Bollin, C., Bolton, E., Bourexis, D., Brister, J.R., Bryant, S.H., Canese, K., Charowhas, C., Clark, K., DiCuccio, M., Dondoshansky, I., Feolo, M., Funk, K., Geer, L.Y., Gorelenkov, V., Hlavina, W., Hoepfner, M., Holmes, B., Johnson, M., Khotomlianski, V., Kimchi, A., Kimelman, M., Kitts, P., Klimke, W., Krasnov, S., Kuznetsov, A., Landrum, M.J., Landsman, D., Lee, J.M., Lipman, D.J., Lu, Z., Madden, T.L., Madej, T., Marchler-Bauer, A., Karsch-Mizrachi, I., Murphy, T., Orris, R., Ostell, J., O'Sullivan, C., Palanigobu, V., Panchenko, A.R., Phan, L., Pruitt, K.D., Rodarmer, K., Rubinstein, W., Sayers, E.W., Schneider, V., Schoch, C.L., Schuler, G.D., Sherry, S.T., Sirotkin, K., Siyan, K., Slotta, D., Soboleva, A., Soussov, V., Starchenko, G., Tatusova, T.A., Todorov, K., Trawick, B.W., Vakarov, D., Wang, Y., Ward, M., Wilbur, W.J., Yaschenko, E., Zbicz, K., 2017. Database Resources of the National Center for Biotechnology Information. *Nucleic Acids Res.* 45, D12–D17. <https://doi.org/10.1093/nar/gkw1071>
- Aldini, G., Altomare, A., Baron, G., Vistoli, G., Carini, M., Borsani, L., Sergio, F., 2018. N-Acetylcysteine as an antioxidant and disulphide breaking agent: the reasons why. *Free Radic. Res.* 52, 751–762. <https://doi.org/10.1080/10715762.2018.1468564>
- Ángeles Esteban, M., Cerezuela, R., 2015. Fish mucosal immunity: skin BT - Mucosal Health in Aquaculture, Mucosal Health in Aquaculture. Elsevier Inc. <https://doi.org/10.1016/B978-0-12-417186-2/00004-2>
- Arnér, E.S.J., Holmgren, A., 2000. Physiological functions of thioredoxin and thioredoxin reductase. *Eur. J. Biochem.* 267, 6102–6109. <https://doi.org/10.1046/j.1432-1327.2000.01701.x>
- Atmaca, G., 2004. Antioxidant Effects of Sulfur-Containing Amino Acids. *Yonsei Med. J.* 45, 776. <https://doi.org/10.3349/ymj.2004.45.5.776>
- Bako, B., 2001. Seahorse. *Med. J. Aust.* 175, 628. <https://doi.org/10.3941/jrcr.v6i6.1170>
- Begas, P., Staudacher, V., Deponte, M., 2015. Systematic re-evaluation of the bis(2-hydroxyethyl)disulfide (HEDS) assay reveals an alternative mechanism and activity of glutaredoxins. *Chem. Sci.* 6, 3788–3796. <https://doi.org/10.1039/C5SC01051A>
- Belcastro, E., Gaucher, C., Corti, A., Leroy, P., Lartaud, I., Pompella, A., 2017. Regulation

- of protein function by S-nitrosation and S-glutathionylation: processes and targets in cardiovascular pathophysiology. *Biol. Chem.* 398, 1267–1293.
<https://doi.org/10.1515/hsz-2017-0150>
- Berndt, C., Lillig, C.H., Holmgren, A., 2008. Thioredoxins and glutaredoxins as facilitators of protein folding. *Biochim. Biophys. Acta - Mol. Cell Res.* 1783, 641–650. <https://doi.org/10.1016/j.bbamcr.2008.02.003>
- Berndt, C., Lillig, C.H., Holmgren, A., 2006. Thiol-based mechanisms of the thioredoxin and glutaredoxin systems: implications for diseases in the cardiovascular system. *AJP Hear. Circ. Physiol.* 292, H1227–H1236. <https://doi.org/10.1152/ajpheart.01162.2006>
- Berndt, C., Poschmann, G., Stühler, K., Holmgren, A., Bräutigam, L., 2014. Zebrafish heart development is regulated via glutaredoxin 2 dependent migration and survival of neural crest cells. *Redox Biol.* 2, 673–678.
<https://doi.org/10.1016/j.redox.2014.04.012>
- Biasini, M., Bienert, S., Waterhouse, A., Arnold, K., Studer, G., Schmidt, T., Kiefer, F., Cassarino, T.G., Bertoni, M., Bordoli, L., Schwede, T., 2014. SWISS-MODEL: Modelling protein tertiary and quaternary structure using evolutionary information. *Nucleic Acids Res.* 42, 252–258. <https://doi.org/10.1093/nar/gku340>
- Bick, J.-A., Aslund, F., Chen, Y., Leustek, T., 1998. Glutaredoxin function for the carboxyl-terminal domain of the plant-type 5'-adenylylsulfate reductase. *Proc. Natl. Acad. Sci.* 95, 8404–8409. <https://doi.org/10.1073/pnas.95.14.8404>
- Brautigam, L., Jensen, L.D.E., Poschmann, G., Nystrom, S., Bannenberg, S., Dreij, K., Lepka, K., Prozorovski, T., Montano, S.J., Aktas, O., Uhlen, P., Stuhler, K., Cao, Y., Holmgren, A., Berndt, C., 2013. Glutaredoxin regulates vascular development by reversible glutathionylation of sirtuin 1. *Proc. Natl. Acad. Sci.* 110, 20057–20062.
<https://doi.org/10.1073/pnas.1313753110>
- Bräutigam, L., Johansson, C., Kubsch, B., McDonough, M.A., Bill, E., Holmgren, A., Berndt, C., 2013. An unusual mode of iron-sulfur-cluster coordination in a teleost glutaredoxin. *Biochem. Biophys. Res. Commun.* 436, 491–496.
<https://doi.org/10.1016/j.bbrc.2013.05.132>
- Brautigam, L., Schutte, L.D., Godoy, J.R., Prozorovski, T., Gellert, M., Hauptmann, G., Holmgren, A., Lillig, C.H., Berndt, C., 2011. Vertebrate-specific glutaredoxin is essential for brain development. *Proc. Natl. Acad. Sci.* 108, 20532–20537.
<https://doi.org/10.1073/pnas.1110085108>
- Browne, R.K., Baker, J.L., Connolly, R.M., 2008. Syngnathids: Seadragons, seahorses, and pipefishes of Gulf St Vincent, in: *Natural History of Gulf St Vincent*. p. 15.
- Bustin, S.A., Benes, V., Garson, J.A., Hellems, J., Huggett, J., Kubista, M., Mueller, R., Nolan, T., Pfaffl, M.W., Shipley, G.L., Vandesompele, J., Wittwer, C.T., 2009. The MIQE Guidelines: Minimum Information for Publication of Quantitative Real-Time PCR Experiments. *Clin. Chem.* 55, 611–622.
<https://doi.org/10.1373/clinchem.2008.112797>
- Campanella, J.J., Bitincka, L., Smalley, J., 2003. MatGAT: An application that generates similarity/identity matrices using protein or DNA sequences. *BMC Bioinformatics* 4, 1–4. <https://doi.org/10.1186/1471-2105-4-29>

- Carmack, M., Kelley, C.J., 1968. Synthesis of optically active Cleland's reagent [(-)-1,4-dithio-L-threitol]. *J. Org. Chem.* 33, 2171–2173. <https://doi.org/10.1021/jo01269a123>
- Chalker, J., Gardiner, D., Kuksal, N., Mailloux, R.J., 2018. Characterization of the impact of glutaredoxin-2 (GRX2) deficiency on superoxide/hydrogen peroxide release from cardiac and liver mitochondria. *Redox Biol.* 15, 216–227. <https://doi.org/10.1016/j.redox.2017.12.006>
- Chantzoura, E., Prinarakis, E., Panagopoulos, D., Mosialos, G., Spyrou, G., 2010. Glutaredoxin-1 regulates TRAF6 activation and the IL-1 receptor/TLR4 signalling. *Biochem. Biophys. Res. Commun.* 403, 335–339. <https://doi.org/10.1016/j.bbrc.2010.11.029>
- Chen, Y., Zhou, Z., Min, W., 2018. Mitochondria, oxidative stress and innate immunity. *Front. Physiol.* 9, 1–10. <https://doi.org/10.3389/fphys.2018.01487>
- Ching, B., Chew, S.F., Ip, Y.K., 2015. Ascorbate synthesis in fishes: A review. *IUBMB Life* 67, 69–76. <https://doi.org/10.1002/iub.1360>
- Collinson, E.J., Grant, C.M., 2003. Role of yeast glutaredoxins as glutathione S-transferases. *J. Biol. Chem.* 278, 22492–22497. <https://doi.org/10.1074/jbc.M301387200>
- Daily, D., Vlamis-Gardikas, A., Offen, D., Mittelmani, L., Melamed, E., Holmgren, A., Barzilai, A., 2001. Glutaredoxin protects cerebellar granule neurons from dopamine-induced apoptosis by activating NF- κ B via Ref-1. *J. Biol. Chem.* 276, 1335–1344. <https://doi.org/10.1074/jbc.M008121200>
- Davis, D.A., Newcomb, F.M., Starke, D.W., Ott, D.E., Mieyal, J.J., Yarchoan, R., 1997. Thioltransferase (glutaredoxin) is detected within HIV-1 and can regulate the activity of glutathionylated HIV-1 protease in vitro. *J. Biol. Chem.* 272, 25935–25940. <https://doi.org/10.1074/jbc.272.41.25935>
- Di Meo, S., Reed, T.T., Venditti, P., Victor, V.M., 2018. Harmful and Beneficial Role of ROS 2017. *Oxid. Med. Cell. Longev.* 2018, 1–2. <https://doi.org/10.1155/2018/5943635>
- Dinarello, C.A., 1997. Interleukin-1. *Cytokine Growth Factor Rev.* 8, 253–265. [https://doi.org/10.1016/S1359-6101\(97\)00023-3](https://doi.org/10.1016/S1359-6101(97)00023-3)
- Division of labour in the fish brain | Max-Planck-Gesellschaft [WWW Document], n.d. URL <https://www.mpg.de/division-of-labour-in-the-fish-brain> (accessed 4.16.19).
- Do, H., Kim, I.S., Jeon, B.W., Lee, C.W., Park, A.K., Wi, A.R., Shin, S.C., Park, H., Kim, Y.S., Yoon, H.S., Kim, H.W., Lee, J.H., 2016. Structural understanding of the recycling of oxidized ascorbate by dehydroascorbate reductase (OsDHAR) from *Oryza sativa* L. *japonica*. *Sci. Rep.* 6, 1–13. <https://doi.org/10.1038/srep19498>
- Duran, B.O.S., Góes, G.A., Zanella, B.T.T., Freire, P.P., Valente, J.S., Salomão, R.A.S., Fernandes, A., Mareco, E.A., Carvalho, R.F., Dal-Pai-Silva, M., 2019. Ascorbic acid stimulates the in vitro myoblast proliferation and migration of pacu (*Piaractus mesopotamicus*). *Sci. Rep.* 9, 1–12. <https://doi.org/10.1038/s41598-019-38536-4>
- Emanuelsson, O., Nielsen, H., Brunak, S., Von Heijne, G., 2000. Predicting subcellular localization of proteins based on their N-terminal amino acid sequence. *J. Mol. Biol.*

- 300, 1005–1016. <https://doi.org/10.1006/jmbi.2000.3903>
- Enoksson, M., Fernandes, A.P., Prast, S., Lillig, C.H., Holmgren, A., Orrenius, S., 2005. Overexpression of glutaredoxin 2 attenuates apoptosis by preventing cytochrome c release. *Biochem. Biophys. Res. Commun.* 327, 774–779. <https://doi.org/10.1016/j.bbrc.2004.12.067>
- Fernandes, A.P., Holmgren, A., 2004. Glutaredoxins: Glutathione-Dependent Redox Enzymes with Functions Far Beyond a Simple Thioredoxin Backup System. *Antioxid. Redox Signal.* 6, 63–74. <https://doi.org/10.1089/152308604771978354>
- Fernando, M.R., Lechner, J.M., Löfgren, S., Gladyshev, V.N., Lou, M.F., 2006. Mitochondrial thioltransferase (glutaredoxin 2) has GSH-dependent and thioredoxin reductase-dependent peroxidase activities in vitro and in lens epithelial cells. *FASEB J.* 20, 2645–2647. <https://doi.org/10.1096/fj.06-5919fje>
- Fernando, M.R., Sumimoto, H., Nanri, H., Kawabata, S. ichiro, Iwanaga, S., Minakami, S., Fukumaki, Y., Takeshige, K., 1994. Cloning and sequencing of the cDNA encoding human glutaredoxin. *BBA - Gene Struct. Expr.* 1218, 229–231. [https://doi.org/10.1016/0167-4781\(94\)90019-1](https://doi.org/10.1016/0167-4781(94)90019-1)
- Foloppe, N., Nilsson, L., 2004. The Glutaredoxin -C-P-Y-C- Motif: Influence of Peripheral Residues. *Structure* 12, 289–300. [https://doi.org/10.1016/S0969-2126\(04\)00021-8](https://doi.org/10.1016/S0969-2126(04)00021-8)
- Fox, T.D., 2012. Mitochondrial protein synthesis, import, and assembly. *Genetics* 192, 1203–1234. <https://doi.org/10.1534/genetics.112.141267>
- Fukasawa, Y., Tsuji, J., Fu, S., Tomii, K., Horton, P., Imai, K., 2015. MitoFates : Improved Prediction of Mitochondrial Targeting Sequences and Their Cleavage 1113–1126. <https://doi.org/10.1074/mcp.M114.043083>
- Gakh, O., Cavadini, P., Isaya, G., 2002. Mitochondrial processing peptidases. *Biochim. Biophys. Acta - Mol. Cell Res.* 1592, 63–77. [https://doi.org/10.1016/S0167-4889\(02\)00265-3](https://doi.org/10.1016/S0167-4889(02)00265-3)
- Gallogly, M.M., Shelton, M.D., Qanungo, S., Pai, H. V., Starke, D.W., Hoppel, C.L., Lesnefsky, E.J., Mieval, J.J., 2010. Glutaredoxin regulates apoptosis in cardiomyocytes via NFkappaB targets Bcl-2 and Bcl-xL: implications for cardiac aging. *Antioxid. Redox Signal.* 12, 1339–1353. <https://doi.org/10.1089/ars.2009.2791>
- Gallogly, M.M., Starke, D.W., Leonberg, A.K., English Ospina, S.M., Mieval, J.J., 2008. Kinetic and mechanistic characterization and versatile catalytic properties of mammalian glutaredoxin 2: Implications for intracellular roles. *Biochemistry* 47, 11144–11157. <https://doi.org/10.1021/bi800966v>
- Gao, X.H., Zaffagnini, M., Bedhomme, M., Michelet, L., Cassier-Chauvat, C., Decottignies, P., Lemaire, S.D., 2010. Biochemical characterization of glutaredoxins from *Chlamydomonas reinhardtii*: Kinetics and specificity in deglutathionylation reactions. *FEBS Lett.* 584, 2242–2248. <https://doi.org/10.1016/j.febslet.2010.04.034>
- Gautier, R., Douguet, D., Antony, B., Drin, G., 2008. HELIQUEST: A web server to screen sequences with specific α -helical properties. *Bioinformatics* 24, 2101–2102. <https://doi.org/10.1093/bioinformatics/btn392>

- Gladyshev, V.N., Liu, A., Novoselov, S. V., Krysan, K., Sun, Q.A., Kryukov, V.M., Kryukov, G. V., Lou, M.F., 2001. Identification and Characterization of a New Mammalian Glutaredoxin (Thioltransferase), Grx2. *J. Biol. Chem.* 276, 30374–30380. <https://doi.org/10.1074/jbc.M100020200>
- González-Fernández, R., Gaytán, F., Martínez-Galisteo, E., Porras, P., Padilla, C.A., Sánchez Criado, J.E., Bárcena, J.A., 2005. Expression of glutaredoxin (thioltransferase) in the rat ovary during the oestrous cycle and postnatal development. *J. Mol. Endocrinol.* 34, 625–635. <https://doi.org/10.1677/jme.1.01715>
- Grek, C.L., Zhang, J., Manevich, Y., Townsend, D.M., Tew, K.D., 2013. Causes and consequences of cysteine s-glutathionylation. *J. Biol. Chem.* 288, 26497–26504. <https://doi.org/10.1074/jbc.R113.461368>
- Gupta, R., Brunak, S., 2001. MEGA7: Molecular Evolutionary Genetics Analysis Version 7.0 for Bigger Datasets. *Biocomput.* 2002 322[1] R., 310–322. <https://doi.org/10.1093/molbev/msw054>
- Hanschmann, E.-M., Godoy, J.R., Berndt, C., Hudemann, C., Lillig, C.H., 2013a. Thioredoxins, Glutaredoxins, and Peroxiredoxins—Molecular Mechanisms and Health Significance: from Cofactors to Antioxidants to Redox Signaling. *Antioxid. Redox Signal.* 19, 1539–1605. <https://doi.org/10.1089/ars.2012.4599>
- Hanschmann, E.-M., Godoy, J.R., Berndt, C., Hudemann, C., Lillig, C.H., 2013b. Thioredoxins, Glutaredoxins, and Peroxiredoxins—Molecular Mechanisms and Health Significance: from Cofactors to Antioxidants to Redox Signaling. *Antioxid. Redox Signal.* 19, 1539–1605. <https://doi.org/10.1089/ars.2012.4599>
- Haunhorst, P., Berndt, C., Eitner, S., Godoy, J.R., Lillig, C.H., 2010. Characterization of the human monothiol glutaredoxin 3 (PICOT) as iron-sulfur protein. *Biochem. Biophys. Res. Commun.* 394, 372–376. <https://doi.org/10.1016/j.bbrc.2010.03.016>
- Hauwer, D.E., n.d. Identification Infection of Escherichia 244, 6306–6309.
- Herrero, E., Ros, J., Tamarit, J., Bellí, G., 2006. Glutaredoxins in fungi. *Photosynth. Res.* 89, 127–140. <https://doi.org/10.1007/s11120-006-9079-3>
- Holmgren, A., 1985. [68] Glutaredoxin from Escherichia coli and calf thymus. pp. 525–540. [https://doi.org/10.1016/S0076-6879\(85\)13071-5](https://doi.org/10.1016/S0076-6879(85)13071-5)
- Holmgren, A., 1979. Thioredoxin catalyzes the reduction of insulin disulfides by dithiothreitol and dihydrolipoamide. *J. Biol. Chem.* 254, 9627–32. <https://doi.org/10.1079>
- Johansson, C., Lillig, C.H., Holmgren, A., 2004. Human Mitochondrial Glutaredoxin Reduces S-Glutathionylated Proteins with High Affinity Accepting Electrons from Either Glutathione or Thioredoxin Reductase. *J. Biol. Chem.* 279, 7537–7543. <https://doi.org/10.1074/jbc.M312719200>
- Karunakaran, S., Saeed, U., Ramakrishnan, S., Koumar, R.C., Ravindranath, V., 2007. Constitutive expression and functional characterization of mitochondrial glutaredoxin (Grx2) in mouse and human brain. *Brain Res.* 1185, 8–17. <https://doi.org/10.1016/j.brainres.2007.09.019>
- Kaufmann, S.H.E., Dorhoi, A., 2016. Molecular Determinants in Phagocyte-Bacteria

- Interactions. *Immunity* 44, 476–491. <https://doi.org/10.1016/j.immuni.2016.02.014>
- Kenchappa, R.S., Ravindranath, V., 2003. Glutaredoxin is essential for maintenance of brain mitochondrial complex I: studies with MPTP. *FASEB J.* 17, 717–719. <https://doi.org/10.1096/fj.-02>
- Khetrapal, N., 2010. Protein Structure and Function Prediction Using I-TASSER. *Handb. Res. Hum. Cogn. Assist. Technol. Des. Access. Transdiscipl. Perspect.* 96–108. <https://doi.org/10.1002/0471250953.bi0508s52>
- Koldewey, H.J., Martin-Smith, K.M., 2010a. A global review of seahorse aquaculture. *Aquaculture* 302, 131–152. <https://doi.org/10.1016/j.aquaculture.2009.11.010>
- Koldewey, H.J., Martin-Smith, K.M., 2010b. A global review of seahorse aquaculture. *Aquaculture* 302, 131–152. <https://doi.org/10.1016/j.aquaculture.2009.11.010>
- Kumar, S., Stecher, G., Tamura, K., 2016. MEGA7: Molecular Evolutionary Genetics Analysis Version 7.0 for Bigger Datasets. *Mol. Biol. Evol.* 33, 1870–1874. <https://doi.org/10.1093/molbev/msw054>
- La Camera, S., L’Haridon, F., Astier, J., Zander, M., Abou-Mansour, E., Page, G., Thurow, C., Wendehenne, D., Gatz, C., Métraux, J.P., Lamotte, O., 2011. The glutaredoxin ATGRXS13 is required to facilitate *Botrytis cinerea* infection of *Arabidopsis thaliana* plants. *Plant J.* 68, 507–519. <https://doi.org/10.1111/j.1365-313X.2011.04706.x>
- Lenaz, G., Fato, R., Genova, M.L., Bergamini, C., Bianchi, C., Biondi, A., 2006. Mitochondrial Complex I: Structural and functional aspects. *Biochim. Biophys. Acta - Bioenerg.* 1757, 1406–1420. <https://doi.org/10.1016/j.bbabi.2006.05.007>
- Lepage, V., Young, J., Dutton, C.J., Crawshaw, G., Paré, J.A., Kummrow, M., McLelland, D.J., Huber, P., Young, K., Russell, S., Al-Hussiney, L., Lumsden, J.S., 2015. Diseases of captive yellow seahorse *Hippocampus kuda* Bleeker, pot-bellied seahorse *Hippocampus abdominalis* Lesson and weedy seadragon *Phyllopteryx taeniolatus* (Lacépède). *J. Fish Dis.* 38, 439–450. <https://doi.org/10.1111/jfd.12254>
- Li, W., Cowley, A., Uludag, M., Gur, T., McWilliam, H., Squizzato, S., Park, Y.M., Buso, N., Lopez, R., 2015. The EMBL-EBI bioinformatics web and programmatic tools framework. *Nucleic Acids Res.* 43, W580–W584. <https://doi.org/10.1093/nar/gkv279>
- Lillig, C.H., Berndt, C., Holmgren, A., 2008. Glutaredoxin systems. *Biochim. Biophys. Acta - Gen. Subj.* 1780, 1304–1317. <https://doi.org/10.1016/j.bbagen.2008.06.003>
- Livak, K.J., Schmittgen, T.D., 2001. Analysis of relative gene expression data using real-time quantitative PCR and the 2- $\Delta\Delta$ CT method. *Methods* 25, 402–408. <https://doi.org/10.1006/meth.2001.1262>
- Liyanage, D.S., Omeke, W.K.M., Godahewa, G.I., Lee, J., 2018. Molecular characterization of thioredoxin-like protein 1 (TXNL1) from big-belly seahorse *Hippocampus abdominalis* in response to immune stimulation. *Fish Shellfish Immunol.* 75, 181–189. <https://doi.org/10.1016/j.fsi.2018.02.009>
- Llorente, C., Schnabl, B., 2016. Fast-Track Clearance of Bacteria from the Liver. *Cell Host Microbe* 20, 1–2. <https://doi.org/10.1016/j.chom.2016.06.012>

- Lo Conte, M., Carroll, K.S., 2013. The redox biochemistry of protein sulfenylation and sulfinylation. *J. Biol. Chem.* 288, 26480–26488. <https://doi.org/10.1074/jbc.R113.467738>
- Lourie, S. a, Foster, S.J., Cooper, E.W.T., Vincent, A.C.J., 2004. *A Guide to the Identification of Seahorses*, North.
- Lu, Y.C., Yeh, W.C., Ohashi, P.S., 2008. LPS/TLR4 signal transduction pathway. *Cytokine* 42, 145–151. <https://doi.org/10.1016/j.cyto.2008.01.006>
- Lundberg, M., Johansson, C., Chandra, J., Enoksson, M., Jacobsson, G., Ljung, J., Johansson, M., Holmgren, A., 2001. Cloning and Expression of a Novel Human Glutaredoxin (Grx2) with Mitochondrial and Nuclear Isoforms. *J. Biol. Chem.* 276, 26269–26275. <https://doi.org/10.1074/jbc.M011605200>
- Marchler-Bauer, A., Derbyshire, M.K., Gonzales, N.R., Lu, S., Chitsaz, F., Geer, L.Y., Geer, R.C., He, J., Gwadz, M., Hurwitz, D.I., Lanczycki, C.J., Lu, F., Marchler, G.H., Song, J.S., Thanki, N., Wang, Z., Yamashita, R.A., Zhang, D., Zheng, C., Bryant, S.H., 2015. CDD: NCBI's conserved domain database. *Nucleic Acids Res.* 43, D222–D226. <https://doi.org/10.1093/nar/gku1221>
- Martin, J.L., 1995. Thioredoxin -a fold for all reasons. *Structure* 3, 245–250. [https://doi.org/10.1016/S0969-2126\(01\)00154-X](https://doi.org/10.1016/S0969-2126(01)00154-X)
- May, J.M., Mendiratta, S., Hill, K.E., Burk, R.F., 1997. Reduction of dehydroascorbate to ascorbate by the selenoenzyme thioredoxin reductase. *J. Biol. Chem.* 272, 22607–22610. <https://doi.org/10.1074/jbc.272.36.22607>
- Mieyal, J.J., Gravina, S.A., 1993. Thioltransferase Is a Specific Glutathionyl Mixed Disulfide Oxidoreductase. *Biochemistry* 32, 3368–3376. <https://doi.org/10.1021/bi00064a021>
- Minasyan, H., 2014. Erythrocyte and blood antibacterial defense. *Eur. J. Microbiol. Immunol.* 4, 138–143. <https://doi.org/10.1556/EuJMI.4.2014.2.7>
- Mu, C., Wang, Q., Yuan, Z., Zhang, Z., Wang, C., 2012. Identification of glutaredoxin 1 and glutaredoxin 2 genes from *Venerupis philippinarum* and their responses to benzo[a]pyrene and bacterial challenge. *Fish Shellfish Immunol.* 32, 482–488. <https://doi.org/10.1016/j.fsi.2011.12.001>
- Murata, H., Ihara, Y., Nakamura, H., Yodoi, J., Sumikawa, K., Kondo, T., 2003. Glutaredoxin exerts an antiapoptotic effect by regulating the redox state of Akt. *J. Biol. Chem.* 278, 50226–33. <https://doi.org/10.1074/jbc.M310171200>
- Oh, M., Umasuthan, N., Elvitigala, D.A.S., Wan, Q., Jo, E., Ko, J., Noh, G.E., Shin, S., Rho, S., Lee, J., 2016. First comparative characterization of three distinct ferritin subunits from a teleost: Evidence for immune-responsive mRNA expression and iron depriving activity of seahorse (*Hippocampus abdominalis*) ferritins. *Fish Shellfish Immunol.* 49, 450–460. <https://doi.org/10.1016/j.fsi.2015.12.039>
- Okonechnikov, K., Golosova, O., Fursov, M., Varlamov, A., Vaskin, Y., Efremov, I., German Grehov, O.G., Kandrov, D., Rasputin, K., Syabro, M., Tleukenov, T., 2012. Unipro UGENE: A unified bioinformatics toolkit. *Bioinformatics* 28, 1166–1167. <https://doi.org/10.1093/bioinformatics/bts091>

- Ouchi, N., Walsh, K., 2012. Cardiovascular and metabolic regulation by the adiponectin/C1q/tumor necrosis factor-related protein family of proteins. *Circulation* 125, 3066–3068. <https://doi.org/10.1161/CIRCULATIONAHA.112.114181>
- Owczarzy, R., Tataurov, A. V, Wu, Y., Manthey, J.A., McQuisten, K.A., Almagbrazi, H.G., Pedersen, K.F., Lin, Y., Garretson, J., McEntaggart, N.O., Sailor, C.A., Dawson, R.B., Peek, A.S., 2008. IDT SciTools: a suite for analysis and design of nucleic acid oligomers. *Nucleic Acids Res.* 36, W163-9. <https://doi.org/10.1093/nar/gkn198>
- Pagni, M., Ioannidis, V., Cerutti, L., Zahn-Zabal, M., Jongeneel, C.V., Hau, J., Martin, O., Kuznetsov, D., Falquet, L., 2007. MyHits: Improvements to an interactive resource for analyzing protein sequences. *Nucleic Acids Res.* 35, 433–437. <https://doi.org/10.1093/nar/gkm352>
- Papov, V. V, Gravina, S. a, Mielal, J.J., Biemann, K., 1994. The primary structure and properties of thioltransferase (glutaredoxin) from human red blood cells. *Protein Sci.* 3, 428–434. <https://doi.org/10.1002/pro.5560030307>
- Passantino, L., Cianciotta, A., Jirillo, E., Altamura, M., Passantino, G.F., Tafaro, A., Patruno, R., 2002. Fish Immunology. I. Binding and Engulfment of *Candida Albicans* By Erythrocytes of Rainbow Trout (*Salmo Gairdneri* Richardson) . *Immunopharmacol. Immunotoxicol.* 24, 665–678. <https://doi.org/10.1081/iph-120016050>
- Peltoniemi, M., 2007. Mechanism of Action of the Glutaredoxins and Their Role in Human Lung Diseases.
- Petersen, T.N., Brunak, S., Von Heijne, G., Nielsen, H., 2011. SignalP 4.0: Discriminating signal peptides from transmembrane regions. *Nat. Methods* 8, 785–786. <https://doi.org/10.1038/nmeth.1701>
- Pourcelot, M., Arnoult, D., 2014. Mitochondrial dynamics and the innate antiviral immune response. *FEBS J.* 281, 3791–3802. <https://doi.org/10.1111/febs.12940>
- Powers, S.K., Ji, L.L., Kavazis, A.N., Jackson, M.J., 2014. Reactive Oxygen Species: Impact on Skeletal Muscle. *Crit Rev Biomed Eng* 1, 941–69. <https://doi.org/10.1002/cphy.c100054.REACTIVE>
- Rajagopal, I., Ahn, B.Y., Moss, B., Mathews, C.K., 1995. Roles of vaccinia virus ribonucleotide reductase and glutaredoxin in DNA precursor biosynthesis. *J. Biol. Chem.* 270, 27415–27418. <https://doi.org/10.1074/jbc.270.46.27415>
- Ray, P.D., Huang, B.-W., Tsuji, Y., 2012. Reactive oxygen species (ROS) homeostasis and redox regulation in cellular signaling. *Cell Signal* 24, 981–990. <https://doi.org/10.1016/j.cellsig.2012.01.008.Reactive>
- Reynaert, N.L., Vliet, A. Van Der, Guala, A.S., McGovern, T., Hristova, M., Pantano, C., Heintz, N.H., Heim, J., Ho, Y.-S., Matthews, D.E., Wouters, E.F.M., Janssen-Heininger, Y.M.W., van der Vliet, A., Guala, A.S., McGovern, T., Hristova, M., Pantano, C., Heintz, N.H., Heim, J., Ho, Y.-S., Matthews, D.E., Wouters, E.F.M., Janssen-Heininger, Y.M.W., 2006. Dynamic redox control of NF- kappa B through of inhibitory kappa B kinase ^α. *Proc. Natl. Acad. Sci. U. S. A.* 103, 13086–91. <https://doi.org/10.1073/pnas.0603290103>

- Richards, R., 1996. The role of erythrocytes in the inactivation of free radicals. *Aust. J. Med. Sci.* 17, 163. [https://doi.org/10.1016/S0306-9877\(98\)90206-7](https://doi.org/10.1016/S0306-9877(98)90206-7)
- Sa, J.-H., Kim, K., Lim, C.-J., 1997. Purification and Characterization of Glutaredoxin from *Cryptococcus neoformans*. *Mol. Cells* 7, 655–660.
- Selles, B., Rouhier, N., Chibani, K., Couturier, J., Gama, F., Jacquot, J.P., 2009. Chapter 13 Glutaredoxin. The Missing Link Between Thiol-Disulfide Oxidoreductases and Iron Sulfur Enzymes, 1st ed, *Advances in Botanical Research*. Elsevier Ltd. [https://doi.org/10.1016/S0065-2296\(10\)52013-5](https://doi.org/10.1016/S0065-2296(10)52013-5)
- Sievers, F., Wilm, A., Dineen, D., Gibson, T.J., Karplus, K., Li, W., Lopez, R., McWilliam, H., Remmert, M., Söding, J., Thompson, J.D., Higgins, D.G., 2011. Fast, scalable generation of high-quality protein multiple sequence alignments using Clustal Omega. *Mol. Syst. Biol.* 7. <https://doi.org/10.1038/msb.2011.75>
- Silverman, R.B., 2000. *Enzyme Kinetics.pdf*. *Org. Chem. Enzym. React.*
- Stahl, R.L., Liebes, L.F., Farber, C.M., Silber, R., 1983. A spectrophotometric assay for dehydroascorbate reductase. *Anal. Biochem.* 131, 341–344. [https://doi.org/10.1016/0003-2697\(83\)90180-X](https://doi.org/10.1016/0003-2697(83)90180-X)
- Starke, D.W., Chock, P.B., Mieyal, J.J., 2003. Glutathione-thiyl radical scavenging and transferase properties of human glutaredoxin (thioltransferase): Potential role in redox signal transduction. *J. Biol. Chem.* 278, 14607–14613. <https://doi.org/10.1074/jbc.M210434200>
- Stavreus-Evers, A., Masironi, B., Landgren, B.M., Holmgren, A., Eriksson, H., Sahlin, L., 2002. Immunohistochemical localization of glutaredoxin and thioredoxin in human endometrium: a possible association with pinopodes. *Mol Hum Reprod* 8, 546–551.
- Sugino, N., 2005. Reactive oxygen species in ovarian physiology. *Reprod. Med. Biol.* 4, 31–44. <https://doi.org/10.1111/j.1447-0578.2005.00086.x>
- Takagi, Y., Nakamura, T., Nishiyama, A., Nozaki, K., Tanaka, T., Hashimoto, N., Yodoi, J., 1999. Localization of glutaredoxin (thioltransferase) in the rat brain and possible functional implications during focal ischemia. *Biochem. Biophys. Res. Commun.* 258, 390–394. <https://doi.org/10.1006/bbrc.1999.0646>
- Terada, T., Oshida, T., Nishimura, M., Maeda, H., Hara, T., Hosomi, S., Mizoguchi, T., Nishihara, T., 1992. Study on human erythrocyte thioltransferase: comparative characterization with bovine enzyme and its physiological role under oxidative stress. *J Biochem* 111, 688–692.
- Titran, A.S., 1982. The Structure of Partially Oxygenated Hemoglobin 257, 163–168.
- Vincent, A.C.J., 1996. The International Trade in Seahorses. *TRAFFIC Int.* 163. <https://doi.org/10.1002/aqc.2493>
- Vlamiš-Gardikas, A., Åslund, F., Spyrou, G., Bergman, T., Holmgren, A., 1997. Cloning, overexpression, and characterization of glutaredoxin 2, an atypical glutaredoxin from *Escherichia coli*. *J. Biol. Chem.* 272, 11236–11243. <https://doi.org/10.1074/jbc.272.17.11236>
- Vlamiš-Gardikas, A., Holmgren, A., 2002. Thioredoxin and glutaredoxin isoforms.

- Methods Enzymol. 347, 286–296. [https://doi.org/10.1016/S0076-6879\(02\)47028-0](https://doi.org/10.1016/S0076-6879(02)47028-0)
- Weiss, M., Steiner, D.F., Philipson, L.H., 2000. Insulin Biosynthesis, Secretion, Structure, and Structure-Activity Relationships, Endotext. MDText.com, Inc. <https://doi.org/25905258>
- Wells, W.W., Xu, D.P., Yang, Y., Rocque, P.A., 1990. Mammalian thioltransferase (glutaredoxin) and protein disulfide isomerase have dehydroascorbate reductase activity. *J. Biol. Chem.* 265, 15361–15364.
- West, A.P., Brodsky, I.E., Rahner, C., Woo, D.K., Erdjument-Bromage, H., Tempst, P., Walsh, M.C., Choi, Y., Shadel, G.S., Ghosh, S., 2011. TLR signalling augments macrophage bactericidal activity through mitochondrial ROS. *Nature* 472, 476–480. <https://doi.org/10.1038/nature09973>
- Wilkins, M.R., Gasteiger, E., Bairoch, A., Sanchez, J.C., Williams, K.L., Appel, R.D., Hochstrasser, D.F., 1999. Protein identification and analysis tools in the ExPASy server. *Methods Mol. Biol.* 112, 531–52. <https://doi.org/10.1385/1592598900>
- Wilson, J.X., Wilson, J.X., 2002. The physiological role of dehydroascorbic acid. *FEBS Lett.* 527, 5–9. [https://doi.org/10.1016/S0014-5793\(02\)03167-8](https://doi.org/10.1016/S0014-5793(02)03167-8)
- Woods, C., 2007. Aquaculture of the big-bellied seahorse *Hippocampus abdominalis* Lesson 1827 (Teleostei: Syngnathidae). Thesis.
- Woods, C.M.C., 2003. Growth and survival of juvenile seahorse *Hippocampus abdominalis* reared on live, frozen and artificial foods. *Aquaculture* 220, 287–298. [https://doi.org/10.1016/S0044-8486\(02\)00227-2](https://doi.org/10.1016/S0044-8486(02)00227-2)
- Wu, H., Lin, L., Giblin, F., Ho, Y.-S., Lou, M.F., 2011. Glutaredoxin 2 knockout increases sensitivity to oxidative stress in mouse lens epithelial cells. *Free Radic. Biol. Med.* 51, 2108–17. <https://doi.org/10.1016/j.freeradbiomed.2011.09.011>
- Wu, H., Xing, K., Lou, M.F., 2010. Glutaredoxin 2 prevents H₂O₂-induced cell apoptosis by protecting complex I activity in the mitochondria. *Biochim. Biophys. Acta - Bioenerg.* 1797, 1705–1715. <https://doi.org/10.1016/j.bbabi.2010.06.003>
- Yang, C.-S., Kim, J.-J., Lee, S.J., Hwang, J.H., Lee, C.-H., Lee, M.-S., Jo, E.-K., 2013. TLR3-Triggered Reactive Oxygen Species Contribute to Inflammatory Responses by Activating Signal Transducer and Activator of Transcription-1. *J. Immunol.* 190, 6368–6377. <https://doi.org/10.4049/jimmunol.1202574>
- Zaffagnini, M., Michelet, L., Massot, V., Trost, P., Lemaire, S.D., 2008. Biochemical characterization of glutaredoxins from *Chlamydomonas reinhardtii* reveals the unique properties of a chloroplasmic CGFS-type glutaredoxin. *J. Biol. Chem.* 283, 8868–8876. <https://doi.org/10.1074/jbc.M709567200>
- Zahedi Avval, F., Holmgren, A., 2009. Molecular mechanisms of thioredoxin and glutaredoxin as hydrogen donors for mammalian S phase ribonucleotide reductase. *J. Biol. Chem.* 284, 8233–8240. <https://doi.org/10.1074/jbc.M809338200>
- Zheng, P.-H., Wang, L., Wang, A.-L., Zhang, X.-X., Ye, J.-M., Wang, D.-M., Sun, J.-F., Li, J.-T., Lu, Y.-P., Xian, J.-A., 2019. cDNA cloning and expression analysis of glutaredoxin (Grx) 2 in the Pacific white shrimp *Litopenaeus vannamei*. *Fish Shellfish Immunol.* 86, 662–671. <https://doi.org/10.1016/j.fsi.2018.12.011>

Zhou, H., Brock, J., Liu, D., Board, P.G., Oakley, A.J., 2012. Structural insights into the dehydroascorbate reductase activity of human omega-class glutathione transferases. *J. Mol. Biol.* 420, 190–203. <https://doi.org/10.1016/j.jmb.2012.04.014>